Influence of liquid core dynamics on rotational modes

Yves Rogister, Bernard Valette

Geophys. J. Int. (2009) **176,** 368–388 doi: 10.1111/j.1365-246X.2008.03996.x

Influence of liquid core dynamics on rotational modes

Yves Rogister[1] and Bernard Valette[2]

[1]*IPGS,* UMR 7516 CNRS-ULP, 5 *rue René Descartes,* F-67084 *Strasbourg, France. E-mail: yves.rogister@eost-u.strasbg.fr*
[2]*Laboratoire de Géophysique Interne et Tectonophysique,* IRD R: 157, *CNRS, Université de Savoie,* F-73376 *Le Bourget du Lac Cedex, France*

Accepted 2008 October 2. Received 2008 September 10; in original form 2008 February 22

SUMMARY

We investigate the influence of the structure and dynamics of the liquid outer core on the Earth's rotational modes through the squared Brunt–Väisälä frequency N^2. The frequencies of the rotational modes are embedded into the continuous spectrum of inertia-gravity modes, which is governed in the complex domain by N^2 and the Earth's rotation speed. By solving the equations for the normal modes of a rotating ellipsoidal elastic earth model and varying the N^2 parameter, we show interactions between pseudo-modes of the liquid core and three rotational modes: the Chandler Wobble (CW), Free Inner Core Nutation (FICN) and Free Core Nutation (FCN). The interaction between pseudo-modes of the outer core and the CW gives rise to avoided crossings, which result in two modes sharing similar displacements, that is, an almost rigid wobble of the mantle and oscillations in the outer core having roughly the same amplitude. The corresponding eigenperiods in a corotating frame of reference are separated by a few days. Avoided crossings are also the only kind of interaction that occurs between core pseudo-modes and the FICN. The coupling is stronger than for the CW, the eigenperiods being a few hundred days apart in an inertial frame of reference. The eigenfunctions are mixed in such a way that the amplitude of the nutation of the inner core is an order of magnitude bigger than the oscillations in the outer core. The FCN shows weaker interactions with the pseudo-modes of the core. However, the shift of its nutation period can reach up to 15 d. Consequently, our results show that the angular momentum approach through Liouville's equations is not sufficient to describe fully the nutational modes.

Key words: Earth rotation variations; Surface waves and free oscilations; Theoretical seismology.

1 INTRODUCTION

On the one hand, we know that, theoretically, there exists at least four rotational (or nutational) normal modes for a rotating ellipsoidal earth model. These are the Free Core Nutation (FCN), Free Inner Core Nutation (FICN), Chandler Wobble (CW) and Inner Core Wobble (ICW). The observational discovery of the CW in polar motion data goes back to the end of the 19th century (Chandler 1891a; Chandler 1891b). The first indirect observations of the FCN in gravity data were obtained in the 1970s by Blum *et al.* (1973) and Lecolazet & Steinmetz (1974), later confirmed by Lecolazet & Melchior (1977), following theoretical models developed by Jeffreys & Vicente (1957) and Molodensky (1961). The period of the FICN deduced from the observation of the forced nutations in VLBI data was reported more recently (Mathews *et al.* 2002). The ICW has not been observed yet (Guo *et al.* 2005a). To simplify, we will also call 'observed periods' the periods that are obtained indirectly through resonance effects in gravity, polar motion, or VLBI data.

A common feature of the FCN, FICN and CW is that their observed periods significantly differ from the theoretical periods computed for elastic earth models in hydrostatic equilibrium. However, the usual explanations for the discrepancies between the observed and theoretical periods are different for each mode. An extra non-hydrostatic flattening of the core–mantle boundary brings the theoretical period of the FCN closer to its observed period (Gwinn *et al.* 1986). The observed period of the FICN is explained by the strong magnetic field at the inner core–outer core boundary (Mathews *et al.* 2002). The influence of the ocean and a high-dissipation mechanism are invoked to reconcile the observed and theoretical periods of the CW (Smith 1981).

Moreover, the single or multiple nature of the CW peak in the spectrum of polar motion has been controversial for over a century. Chandler (1901a,b) himself was the first to suggest that the wobble might be double. Rogister & Valette (2005) collected a series of published values for the CW period from 1974 until 2003. Different analyses of the same data set of polar motion give different results: the CW period may be single, double, multiple, or variable in time. Since that paper has been published, new analyses have been made (Guo *et al.* 2005b; Hu *et al.* 2007; Pan 2007) but no definite conclusion has been reached yet.

On the other hand, much less is known about the normal modes of the liquid core. Most notably, core modes have never been observed.

Their calculation for realistic earth models remains challenging. Ideally, the gravitational, Coriolis, viscous and magnetic forces, as well as the shape of the inner core–outer core and core–mantle boundaries, should be taken into account. Nevertheless, to simplify the problem, we will limit ourselves to rotating ellipsoidal elastic earth models, neglecting viscous and magnetic effects. Except for the planetary modes that we will briefly investigate in Section 4, the existence of isolated eigenfrequencies is not guaranteed. Consequently, the normal modes that we will obtain by truncating the displacement field expanded in a series of spherical harmonics will be called 'pseudo-modes'.

It has been repeatedly suggested (for instance, Rochester *et al.* 1974; Toomre 1974; Smith 1977; Gwinn *et al.* 1986; Lumb & Aldridge 1991) that the nutational modes could be influenced by hypothetical core modes. Wu & Wahr (1997) unsuccessfully searched for interaction between core modes and the CW and FCN of an earth model made up of a rigid mantle and a homogeneous incompressible liquid core, so they concluded that 'it is unlikely that they [the inertial core modes] play an important role in the Earth's rotation'. In this paper, we use Smith's (1974) theoretical approach to compute the frequencies of the normal modes of a rotating, elastic earth model. We vary the structure of the outer core within limits allowed by seismological constraints to show that rotational modes and core pseudo-modes can have close frequencies. We estimate how much the frequencies of the FCN, FICN and CW are modified when this interaction happens. We find that the influence of pseudo-modes is stronger for the FICN than CW and FCN. We show that two interacting modes have similar eigenfunctions, which results from the superposition of the eigenfunctions of both an isolated rotational mode and an isolated core pseudo-mode. The difference between their periods is roughly a few days to 15 d for the CW and FCN, while it can reach up to a few hundred days for the FICN, being understood that the FCN and FICN periods are nutation periods in an absolute frame of reference and the CW period is the wobble period in a frame of reference tied in a prescribed way to the Earth mantle.

The paper is organized as follows. Section 2 is devoted to the description of the normal-modes spectrum of a rotating elastic earth model. It includes the seismic modes, the rotational modes and the inertia-gravity spectrum of the liquid core. In Section 3, we expand the displacement field of the nutational modes in a series of vector spherical harmonics, which we truncate for numerical computation. In Section 4, we first compute the planetary modes, which are toroidal inertial modes. Next, we successively consider the interaction of the CW, FCN and FICN with the inertia-gravity spectrum of the liquid core. In Section 5, we discuss the accuracy of an alternative approach to the study of the rotational modes, which is based on Liouville's equations, and summarize our conclusions.

2 NORMAL MODES SPECTRUM OF A ROTATING ELASTIC EARTH

We consider a rotating earth model having an isotropic linearly elastic constitutive relation and being in hydrostatic equilibrium. To determine the spectrum of its normal modes, we must study the non-linear spectral problem related to the family of operators

$$\boldsymbol{L}(\nu) = -\nu^2 \boldsymbol{I_d} + 2i\nu\boldsymbol{\Omega} \times + \boldsymbol{A}, \tag{1}$$

where $\boldsymbol{I_d}$ is the identity and $\boldsymbol{A}$ is the elastic-gravitational operator (Valette 1986). The spectrum Σ_L of the family $\boldsymbol{L}$ is the set of complex numbers ν for which the operator $\boldsymbol{L}(\nu)$ is not continuously invertible, which means that the equation

$$\boldsymbol{L}(\nu)\mathbf{s} = \mathbf{f}(\nu), \tag{2}$$

where $\mathbf{s}$ is the displacement vector, cannot be correctly solved for all $\mathbf{f}(\nu)$. The point spectrum Σ_p is the set of all the eigenvalues: it is the subset of Σ_L that consists of all the complex numbers ν for which the null space of $\boldsymbol{L}(\nu)$ is not reduced to the null vector, that is, for which there exits a non-null displacement vector $\mathbf{s}$ such that

$$\boldsymbol{L}(\nu)\mathbf{s} = \mathbf{0}. \tag{3}$$

The discrete spectrum Σ_d is the set of all the eigenvalues of finite multiplicity which are isolated in Σ_L. In an infinite-dimensional space, spectrum Σ_L must be clearly distinguished from both the point and discrete spectra. More precisely, it may contain a continuous part with no eigenvalue.

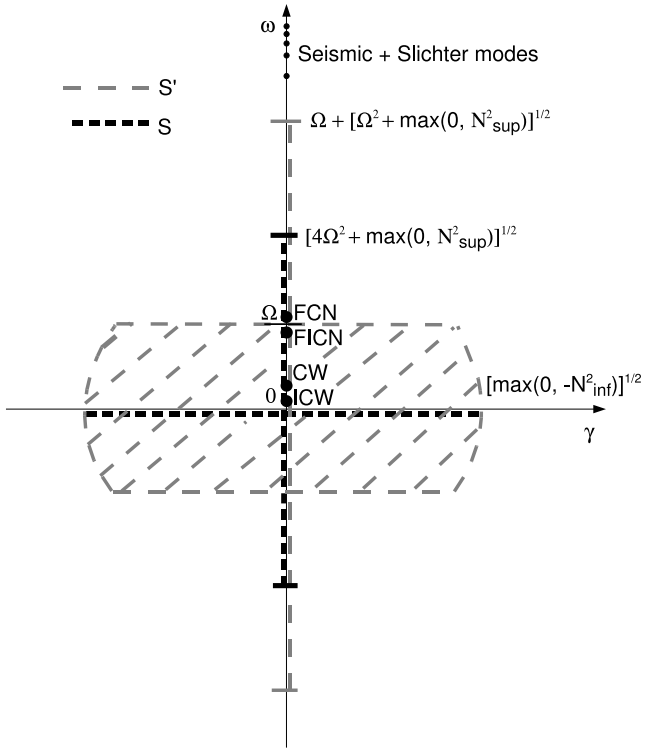

Figure 1. Normal-modes spectrum of a rotating elastic earth model. The abscissa (resp. ordinate) is the imaginary (resp. real) part of the eigenfrequency $\nu = \omega + i\gamma$. The axes are not drawn to scale. N^2 is the squared Brunt–Väisälä frequency defined by eq. (4). The expression max $(0,\ N^2_{\rm sup})$ stands for either 0 or the maximum N^2 value over the liquid core, according to whether N^2 is everywhere negative or not. For PREM, $\Omega + \sqrt{\Omega^2 + N^2_{\rm sup}}$ is 0.1745 mHz (10.00 hr), $\sqrt{4\Omega^2 + N^2_{\rm sup}}$ is 0.1621 mHz (10.77 hr), and $N_{\rm inf}$ is i 0.1703 mHz (i 10.25 hr). Modes that have frequencies on the imaginary axis are purely oscillatory. Modes that have frequencies with a non null real part grow or decay exponentially with time. If they grow with time, they are convective modes. The seismic modes spectrum, which, for PREM, includes the Slichter modes, is discrete. The spectrum Σ related to the liquid core includes S and is included in S': $\mathrm{S} \subseteq \Sigma \subseteq \mathrm{S'}$. The four rotational modes (Free Core Nutation, Free Inner Core Nutation, Chandler Wobble and Inner Core Wobble) are embedded into Σ.

Fig. 1 shows the complex eigenfrequencies $\nu = \omega + i\gamma$ of the normal modes of a rotating elastic earth model in the plane $(\gamma,\ \omega)$. A normal mode with a purely real (resp. purely imaginary) eigenfrequency ω (resp. $i\gamma$) has an associated motion that is oscillatory (resp. exponentially growing or decaying). Ω is the norm of angular

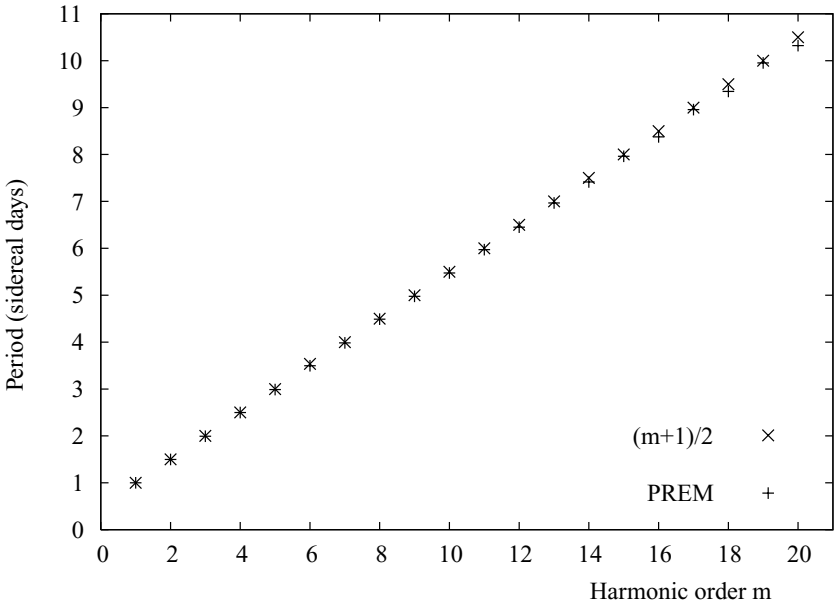

Figure 2. Periods (in sidereal days) of planetary modes of PREM and corresponding eigenperiods $(m + 1)\,\pi/\Omega$ of a non-gravitating, incompressible, and inviscid liquid shell, as a function of harmonic order m. The planetary mode of order 1 is the tilt-over mode. The periods have been computed using a TSTS coupling chain that starts at $\boldsymbol{\tau}_m^m$.

velocity $\boldsymbol{\Omega}$ of the Earth and N^2 is the square of the Brunt–Väisälä frequency defined by

$$N^2 = \mathbf{g} \cdot \left(\frac{\nabla \rho}{\rho} - \frac{\mathbf{g}}{v_p^2} \right), \tag{4}$$

where $\mathbf{g}$ is gravity, ρ is density and v_p is P-wave velocity. N^2 can also be expressed in terms of the stability parameter β defined by

$$\nabla \rho = (1 - \beta) \frac{\rho}{v_p^2} \mathbf{g}, \tag{5}$$

which gives

$$N^2 = -\frac{\beta g^2}{v_p^2}, \tag{6}$$

where g is the norm of $\mathbf{g}$. In a spherically symmetric, chemically homogeneous and single-phase layer, N^2 can be related to the actual gradient of specific entropy or equivalently, to the departure of the actual temperature gradient from the isentropic temperature gradient (Birch 1952; Bullen 1975, pp. 153–156; Valette 1986):

$$N^2 = \alpha_P g \left(\frac{\mathrm{d}\Theta}{\mathrm{d}r} - \left. \frac{\mathrm{d}\Theta}{\mathrm{d}r} \right|_s \right) = \frac{1}{\rho} \left. \frac{\partial \rho}{\partial s} \right|_\Theta g \frac{\mathrm{d}s}{\mathrm{d}r}, \tag{7}$$

r being the radius, $\alpha_P(r)$ being the coefficient of volume expansion at constant pressure, $\Theta(r)$ the temperature and $s(r)$ the specific entropy.

In the complex plane $\nu = (\gamma, \omega)$, the spectrum of a rotating elastic earth model can be divided into three sets: the discrete seismic spectrum, the inertia-gravity spectrum of the liquid outer core and the set of rotational (or nutational) modes.

2.1 Seismic modes

The seismic spectrum corresponds to the discrete part of the spectrum, which means that it is made up of all the eigenfrequencies of finite multiplicity that are isolated in the whole spectrum. Except for the translational modes of the inner core, the so-called Slichter modes, the frequencies (resp. periods) of all the seismic modes are higher (resp. lower) than approximately 0.2999 mHz (resp. 55.6 min). For realistic earth models, the Slichter frequencies (resp. periods) range between 0.040 and 0.056 mHz (resp. 5 and 7 hr). We anticipate that they might be imbedded into the continuous spectrum of the liquid core and, therefore, do not necessarily belong to the discrete spectrum. We will not consider the seismic free oscillations any further.

2.2 Inertia-gravity spectrum of liquid core

The inertia-gravity spectrum Σ of an inviscid liquid core is controlled by the Coriolis and buoyancy forces. Therefore, the relevant parameters are Ω and N^2. Valette (1989a,b) showed that Σ is

Table 1. Upper layers of a modified oceanless PREM model. ρ, V_P and V_S and Q_κ and Q_μ are the density, seismic wave velocities and quality factors, respectively. Values in parentheses are the original PREM values.

Radius (km)	ρ (kg m^{-3})	v_p (m s^{-1})	v_s (m s^{-1})	Q_κ	Q_μ
6346.6	PREM	PREM	PREM	PREM	PREM
6356.0	2800 (2900)	PREM	PREM	PREM	PREM
6368.0	2500 (2600)	PREM	PREM	PREM	PREM
6371.0	2500 (1020)	5800 (1450)	3200 (0)	PREM	600 (∞)

Table 2. Period (in solar days), in a uniformly rotating reference frame, of the CW for four models and three coupling chains. The second and fourth models have a neutrally stratified liquid core ($N^2 = 0$).

Model	TS	TST	TSTS
Oceanless PREM	404.8	402.1	401.5
Oceanless PREM ($N^2 = 0$)	405.3	405.5	405.2
1066 A	402.3	402.3	402.2
1066 A ($N^2 = 0$)	403.3	402.4	402.4

continuous and set bounds on it. More precisely, he showed that S $\subseteq \Sigma \subseteq$ S′, where sets S and S′ of frequencies $\nu = \omega + i\gamma$ are, respectively, defined by

$$\nu = \omega + i\gamma \in$$
$$\mathrm{S} \Longleftrightarrow \begin{cases} \gamma = 0 \quad \text{and } |\omega| \leq \sqrt{4\Omega^2 + \mathrm{Max}(0,\, N^2_{\mathrm{sup}})} \\ \text{or} \\ \omega = 0 \quad \text{and } \gamma^2 \leq \mathrm{Max}(0,\, -N^2_{\mathrm{inf}}) \end{cases} \tag{8}$$

and

$$\nu = \omega + i\gamma \in$$
$$\mathrm{S}' \Longleftrightarrow \begin{cases} \gamma = 0 \quad \text{and } |\omega| \leq \Omega + \sqrt{\Omega^2 + \mathrm{Max}(0,\, N^2_{\mathrm{sup}})} \\ \text{or} \\ |\omega| \leq \Omega \quad \text{and } \omega^2 + \gamma^2 \leq \mathrm{Max}(0,\, -N^2_{\mathrm{inf}}), \end{cases} \tag{9}$$

N^2_{inf} (resp. N^2_{sup}) denoting the minimum (resp. maximum) value of N^2 over the outer core. The three Slichter frequencies, bounded by 0.040 and 0.056 mHz, all belong to the discrete spectrum if

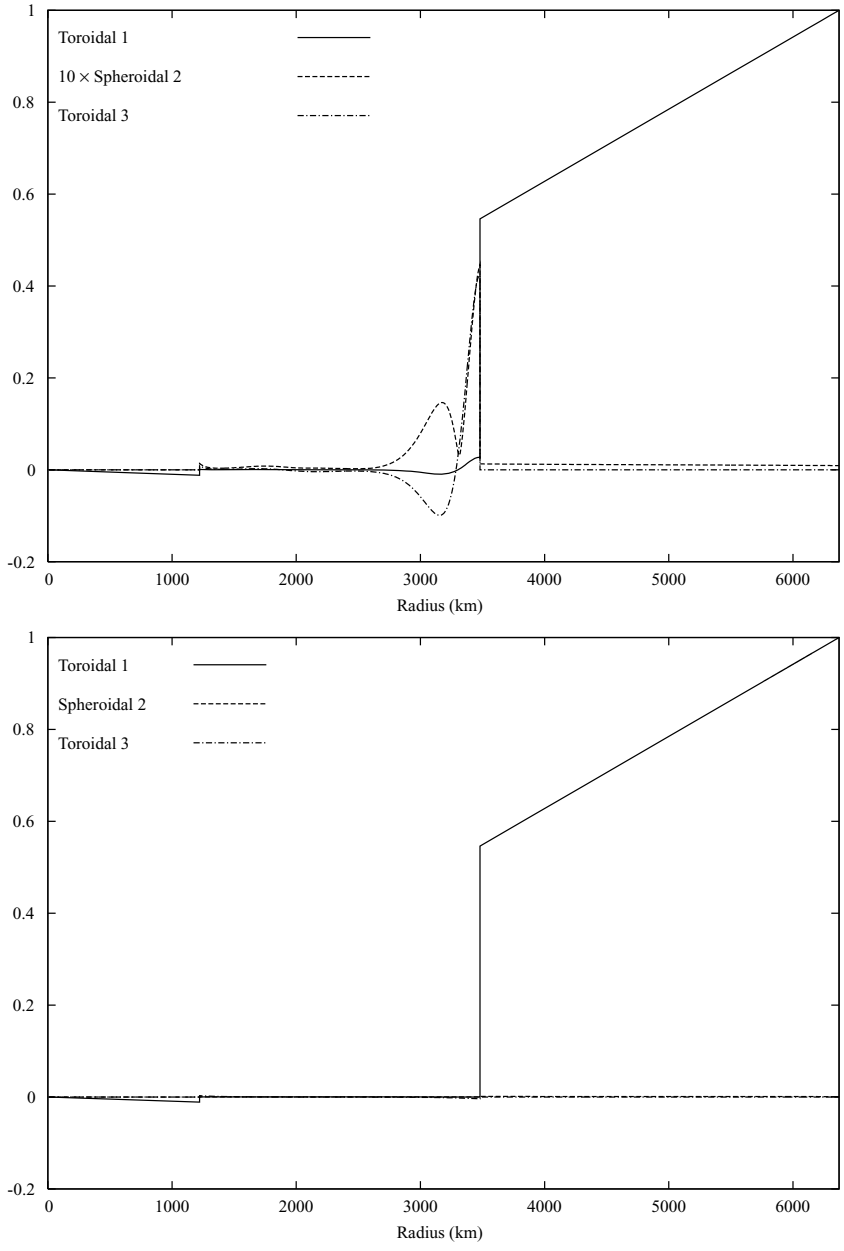

Figure 3. Top panel: theoretical CW for the oceanless version of PREM given in Table 1. Its period is given in Table 2 for different lengths of the coupling chain. The eigendisplacements, computed for a TST coupling chain, are shown as a function of radius. The solid line is the toroidal scalar W_1^{-1}. The degree-2 spheroidal displacement is shown as $\sqrt{2(U_2^{-1})^2 + (V_2^{-1})^2}$. To be visible on the same scale, it is multiplied by 10. The degree-4 spheroidal displacement is of the same order of magnitude but is not shown to keep the figure readable. The motion is dominantly a wobble of the mantle. Bottom panel: theoretical CW for the same oceanless version of PREM that has been further modified so that $N^2 = 0$ in the liquid core.

$N^2_{\rm sup} \leq 2.8 \times 10^{-8}$ rad^2 s^{-2}, whereas they are imbedded into the continuous spectrum if $N^2_{\rm sup} \geq 10^{-7}$ rad^2 s^{-2}.

Spectrum Σ can be entirely determined in the following two cases:

(i) If $\Omega = 0$, Σ is the spectrum of the elastic-gravitational operator. It follows from (8) and (9) that

$$\nu = \omega + i\gamma \in \Sigma = \mathrm{S} = \mathrm{S}' \Longleftrightarrow \begin{cases} \gamma = 0 \quad \text{and} \quad \omega^2 \leq \mathrm{Max}(0,\ N^2_{\rm sup}) \\ \text{or} \\ \omega = 0 \quad \text{and} \quad \gamma^2 \leq \mathrm{Max}(0,\ -N^2_{\rm inf}). \end{cases} \tag{10}$$

Hence we recover Schwarzschild's criterion (Schwarzschild 1906): the stratification is either locally stable or unstable according to whether N^2 is locally positive or negative (Friedman & Schutz 1978; Valette 1986).

(ii) If $N^2 = 0$ everywhere in the fluid, sets (8) and (9) give

$$\nu = \omega + i\gamma \in \Sigma = \mathrm{S} = \mathrm{S}' \Longleftrightarrow \gamma = 0 \text{ and } |\omega| \leq 2\Omega. \tag{11}$$

In particular, this yields the result obtained by Ralston (1973) for the Poincaré problem, which consists in considering a uniform liquid contained in a rigid shell of any shape, neglecting the buoyancy forces, and assuming that the motion is divergence free. For a cylindrical or spherical configuration, Greenspan (1969) calculated the point spectrum, which is the set of eigenfrequencies, for the Poincaré problem. It is everywhere dense in the interval $[-2\Omega, 2\Omega]$. The corresponding modes are called 'inertial modes'. Kudlick (1966) found an implicit solution for the eigenfrequencies of the inertial modes of a contained fluid spheroid.

In the general case, the determination of the point spectrum remains an unsolved problem. The only inertial modes of a fluid

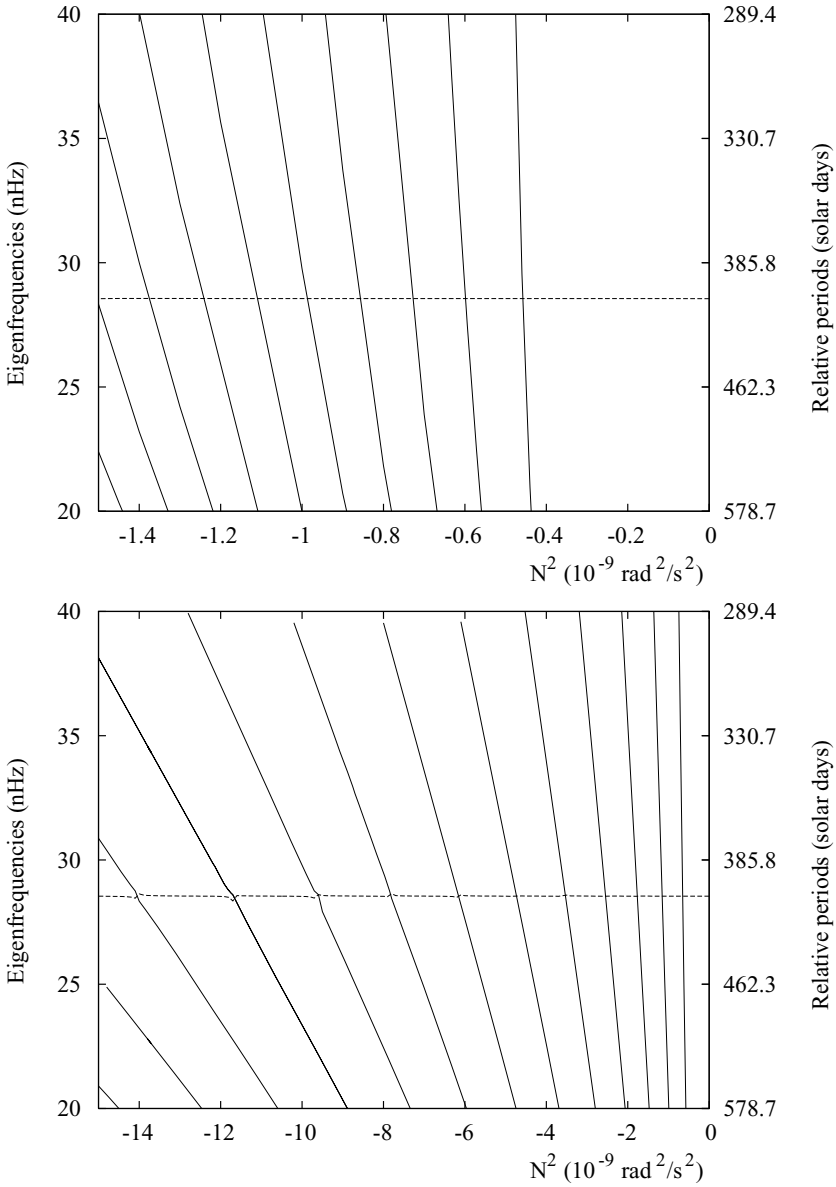

Figure 4. Eigenfrequencies of pseudo-modes (solid lines) and CW (dashed line) as a function of the uniform squared Brunt–Väisälä frequency in the outer core. Pseudo-modes along a branch are characterized by a same number of nodes of the displacement scalars in the outer core. This number is 1 for the first branch on the right. Top panel: TS coupling. Bottom panel: TST coupling. Zooms in on the intersections between the Chandler branch and the third and 19th branches of pseudo-modes in the bottom panel are shown in Fig. 5, where one can actually see that the branches avoid crossing.

spherical shell that are analytically known are purely toroidal modes (Rieutord & Valdaretto 1997) named 'planetary modes' or 'Rossby modes', which are well known in atmospheric and oceanographic dynamics (Longuet-Higgins 1964). We devote Section 4.1 to their description. Numerical investigation by Rieutord *et al.* (2001) of the Poincaré problem suggests that they are the only modes for a spherical shell, thereby extending the conclusion by Aldridge (1975) that there are no regular axisymmetric inertial modes for a spherical shell.

Finally, we mention that a regularization of the problem can be achieved by considering a viscous fluid core. Indeed, the spectrum then becomes discrete, except for 0, which remains an accumulation point in the spectrum.

2.3 Rotational modes

Apart from the tilt-over mode (Smith 1977), a non-spherical rotating earth model *a priori* possesses four rotational modes: the FCN, FICN, CW and ICW. In a uniformly rotating frame of reference, the first two modes have nearly diurnal periods, whereas the CW period is approximately 430 solar days and, as far as the models fairly represent the dynamics of the Earth, the ICW period is likely to be a few thousand days. In that frame, both the FCN and FICN are retrograde modes, whereas both the CW and ICW are prograde modes. In the next section, we expand the displacement field of the nutational modes in spherical harmonics. The CW, FCN and FICN will be separately considered in Section 4.

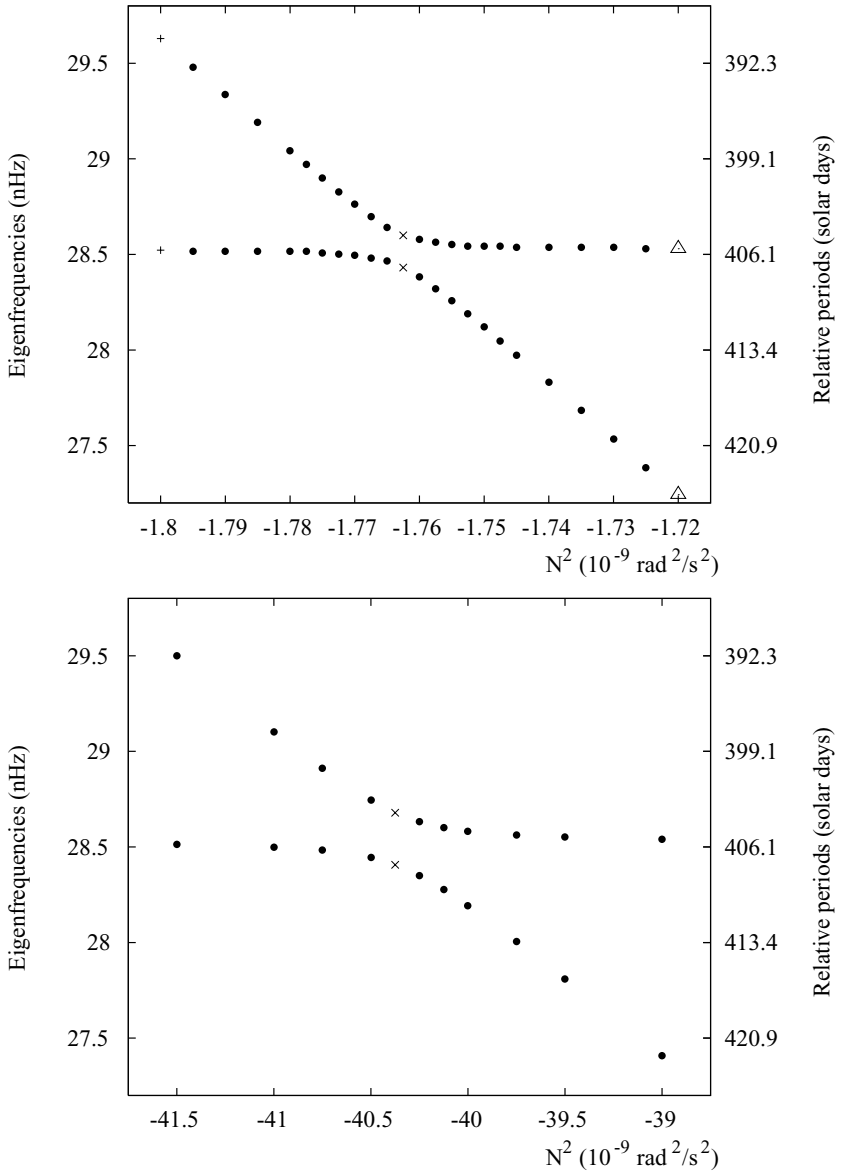

Figure 5. Zooms in on the intersections between the Chandler branch and the thirrd (top panel) and 19th (bottom panel) branches of pseudo-modes in the bottom panel (TST coupling) of Fig. 4. Actually, the branches do not cross but avoid crossing. In some way, they are interrupted in the vicinity of the avoided crossing and the eigenfunctions mix with equal amplitudes. For that reason, we do not connect the dots by solid lines. The eigendisplacements of the modes indicated by + signs are shown in Fig. 6, those indicated by crosses in the top panel are shown in Fig. 7, those indicated by triangles are shown in Fig. 8, and those indicated by crosses in the bottom panel are shown in Fig. 9.

3 DISPLACEMENT FIELD OF ROTATIONAL MODES

To compute the normal modes of a rotating spheroidal earth model, we solve the equations of motion established by Smith (1974) and improved by Schastok (1997), Rogister (2001), Rogister (2003) and Huang *et al.* (2004). We split the displacement field **s**, which is relative to a uniformly rotating reference frame, into a toroidal field $\boldsymbol{\tau}$ and a spheroidal field $\boldsymbol{\sigma}$

$$\mathbf{s} = \boldsymbol{\tau} + \boldsymbol{\sigma}, \tag{12}$$

where

$$\boldsymbol{\sigma} = U\frac{\mathbf{r}}{r} + \frac{\mathbf{r}}{r} \times [\boldsymbol{\nabla} \times (V\,\mathbf{r})] \tag{13}$$

and

$$\boldsymbol{\tau} = \boldsymbol{\nabla} \times (W\,\mathbf{r}) = \mathbf{r} \times \boldsymbol{\nabla} W, \tag{14}$$

r being the position vector. Scalars U, V and W are then decomposed on the basis of complex spherical harmonics $\mathcal{D}_\ell^m(\theta, \varphi)$, where θ and φ are colatitude and longitude, respectively, and $\ell \in \mathbb{N}$ and $m = -\ell, -\ell + 1, \ldots, \ell - 1, \ell$ are the harmonic degree and order, respectively. The normalization adopted for the spherical harmonics is the same as Smith's (1974). The harmonic components U_ℓ^m, $-V_\ell^m/\sqrt{2\ell(\ell+1)}$, and $-iW_\ell^m/\sqrt{2\ell(\ell+1)}$ of U, V and W, respectively, depend on the radius and frequency of the motion. Because of rotation and ellipticity of figure, spheroidal and toroidal displacements of different harmonic degrees couple according to the rules

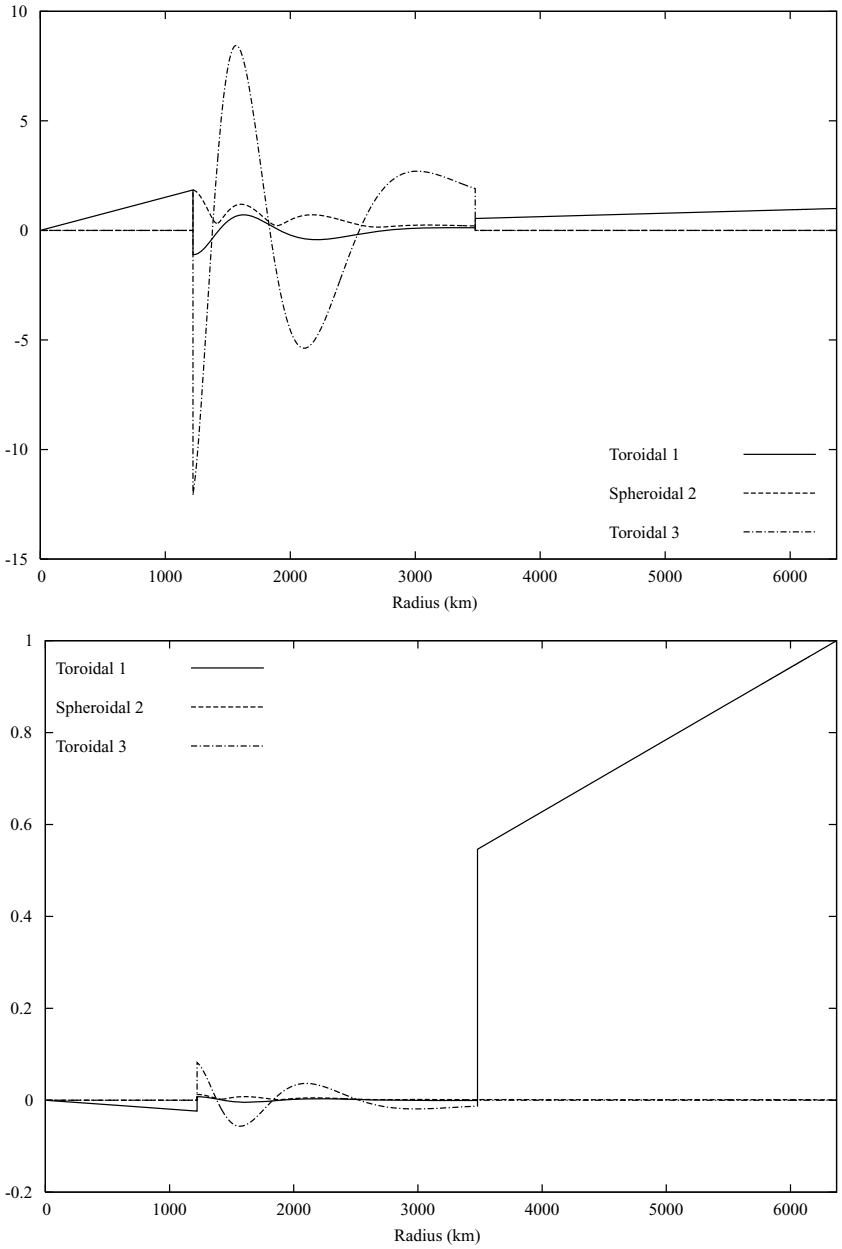

Figure 6. As Fig. 3 for our oceanless PREM model that has been changed so that $N^2 = -1.8 \times 10^{-9}$ rad^2 s^{-2} everywhere in the outer core. The eigenperiods are 390.7 (top panel) and 405.6 (bottom panel) solar days. The corresponding eigenfrequencies are indicated by + signs in Fig. 5. The first mode is dominantly a pseudo-mode of the outer core whereas the second mode is dominantly the CW.

$$\mathbf{s} = \sum_{\ell=|m|,\,|m|+2,\,\ldots}^{\infty} \left(\boldsymbol{\sigma}_\ell^m + \boldsymbol{\tau}_{\ell+1}^m\right) \tag{15}$$

or

$$\mathbf{s} = \sum_{\ell=|m|,\,|m|+2,\,\ldots}^{\infty} \left(\boldsymbol{\tau}_\ell^m + \boldsymbol{\sigma}_{\ell+1}^m\right). \tag{16}$$

Let us consider a system of reference with absolute axis z and relative axes x and y that rotate about the z-axis at absolute angular velocity Ω in the direct sense. In that frame, a nutational mode corresponds to a quasi-rigid rotation about an equatorial axis of at least one of the layers of the Earth, that is, the solid inner core, the liquid outer core or the mantle. Thus, let us also consider an axis $\mathcal{A}$ that uniformly rotates about the z-axis in the equatorial plane xy at relative angular speed ω. In complex notation, the infinitesimal rotation of a mass point about $\mathcal{A}$ is the toroidal motion of degree 1 and order ± 1 given by

$$\boldsymbol{\tau}_1^{\pm 1}(\mathbf{r},\, t) = \boldsymbol{\nabla} \times \left[-\frac{i}{2} W_1^{\pm 1}(r) \mathcal{D}_1^{\pm 1}(\theta,\, \varphi) e^{i\omega t} \mathbf{r}\right] \tag{17}$$

$$= -\frac{i W_1^{\pm 1}(r)}{2\sqrt{2}r} (\mathbf{e}_x \pm i\,\mathbf{e}_y) \times \mathbf{r}\, e^{i\omega t}, \tag{18}$$

where

$$\mathcal{D}_1^{\pm 1}(\theta,\, \varphi) = \pm \frac{1}{\sqrt{2}} \sin\theta e^{\pm i\varphi}, \tag{19}$$

t is time and $\mathbf{e}_x$ and $\mathbf{e}_y$ are unit vectors along the x and y-axes, respectively. The amplitude of the nutation angle is $W_1^{\pm 1}/2\sqrt{2}r$.

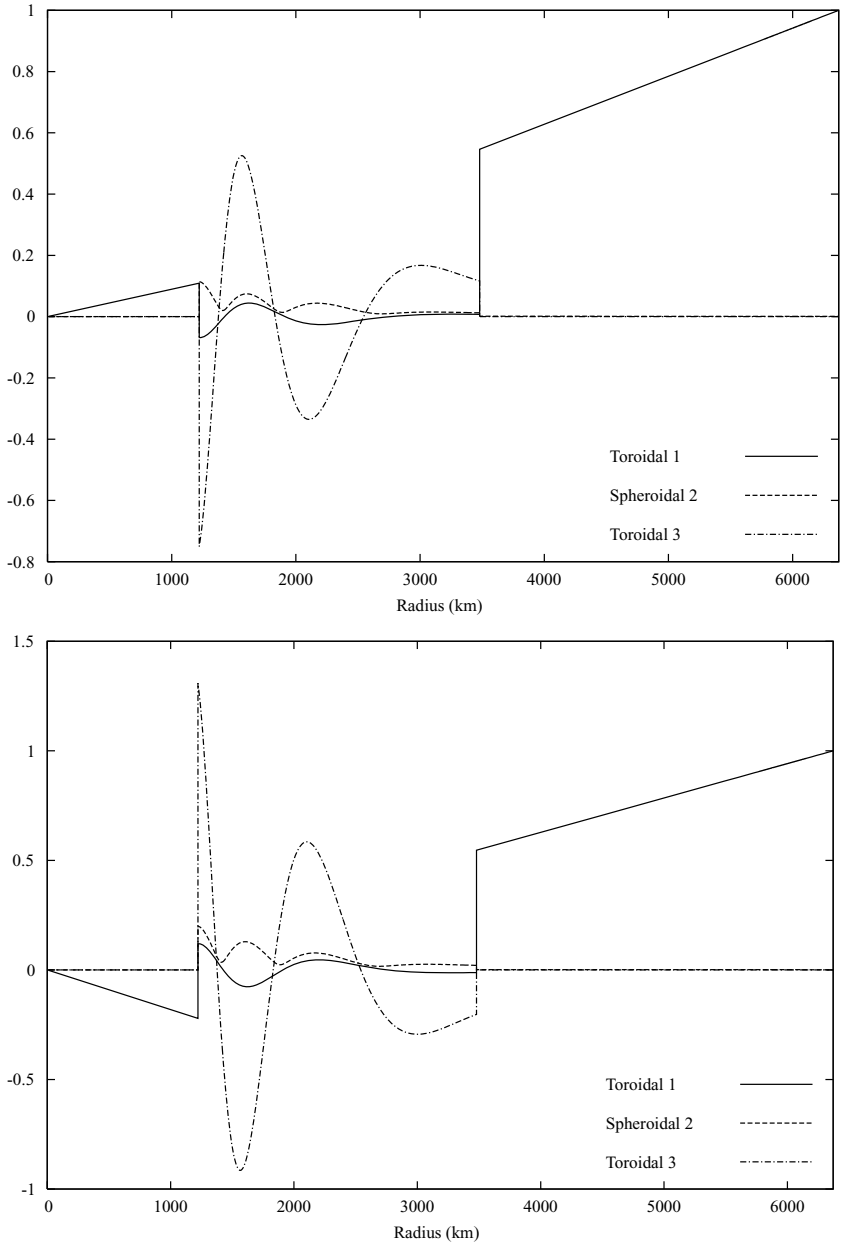

Figure 7. As Fig. 6 for the modes indicated by crosses in the top panel of Fig. 5. $N^2 = -1.7625 \times 10^{-9}$ rad^2 s^{-2} everywhere in the outer core. The eigenperiods are 404.6 (top panel) and 407.1 solar days (bottom panel). Both modes share a similar wobble of the mantle. The amplitude of the oscillations in the outer core is comparable to the wobble amplitude.

Consequently, if $W_1^{\pm 1}$ is a linear function of r, the rotation of the body about $\mathcal{A}$ is rigid. Using our sign convention for the Fourier transform ($e^{i\omega t}$), displacement $\boldsymbol{\tau}_1^1$ (resp. $\boldsymbol{\tau}_1^{-1}$) corresponds to a retrograde (resp. prograde) wobble in the uniformly rotating reference frame. The FCN and FICN involve retrograde wobbles whereas the CW and ICW are prograde wobbles. The FICN and ICW involve a wobble of the inner core, the FCN involves a wobble of the outer core, and the CW involves a wobble of the mantle.

Besides, the Earth deforms as it wobbles. Since the eigendisplacement of a rotational mode can be written

$$\mathbf{s} = \sum_{\ell=1,\,3,\,5,\,\ldots}^{\infty} \left(\boldsymbol{\tau}_\ell^{\pm 1} + \boldsymbol{\sigma}_{\ell+1}^{\pm 1}\right), \tag{20}$$

where

$$\boldsymbol{\tau}_\ell^{\pm 1} = -\frac{i\,W_\ell^{\pm 1}}{\sqrt{2\ell(\ell+1)}}\left(\pm\frac{\mathcal{D}_\ell^{\pm 1}}{\sin\theta}\mathbf{e}_\theta + i\,\frac{\partial \mathcal{D}_\ell^{\pm 1}}{\partial\theta}\mathbf{e}_\varphi\right) e^{i\omega t} \tag{21}$$

and

$$\boldsymbol{\sigma}_\ell^{\pm 1} = \left[U_\ell^{\pm 1}\mathcal{D}_\ell^{\pm 1}\mathbf{e}_r - \frac{V_\ell^{\pm 1}}{\sqrt{2\ell(\ell+1)}}\left(\frac{\partial \mathcal{D}_\ell^{\pm 1}}{\partial\theta}\mathbf{e}_\theta \pm i\,\frac{\mathcal{D}_\ell^{\pm 1}}{\sin\theta}\mathbf{e}_\varphi\right)\right] e^{i\omega t}, \tag{22}$$

the deformation is given by the terms of harmonic degrees ℓ greater than 1, and by the non linear part of $W_1^{\pm 1}$ as a function of r. We make no explicit assumption about the amplitudes of the deformation terms. However, for numerical purposes, series (20)

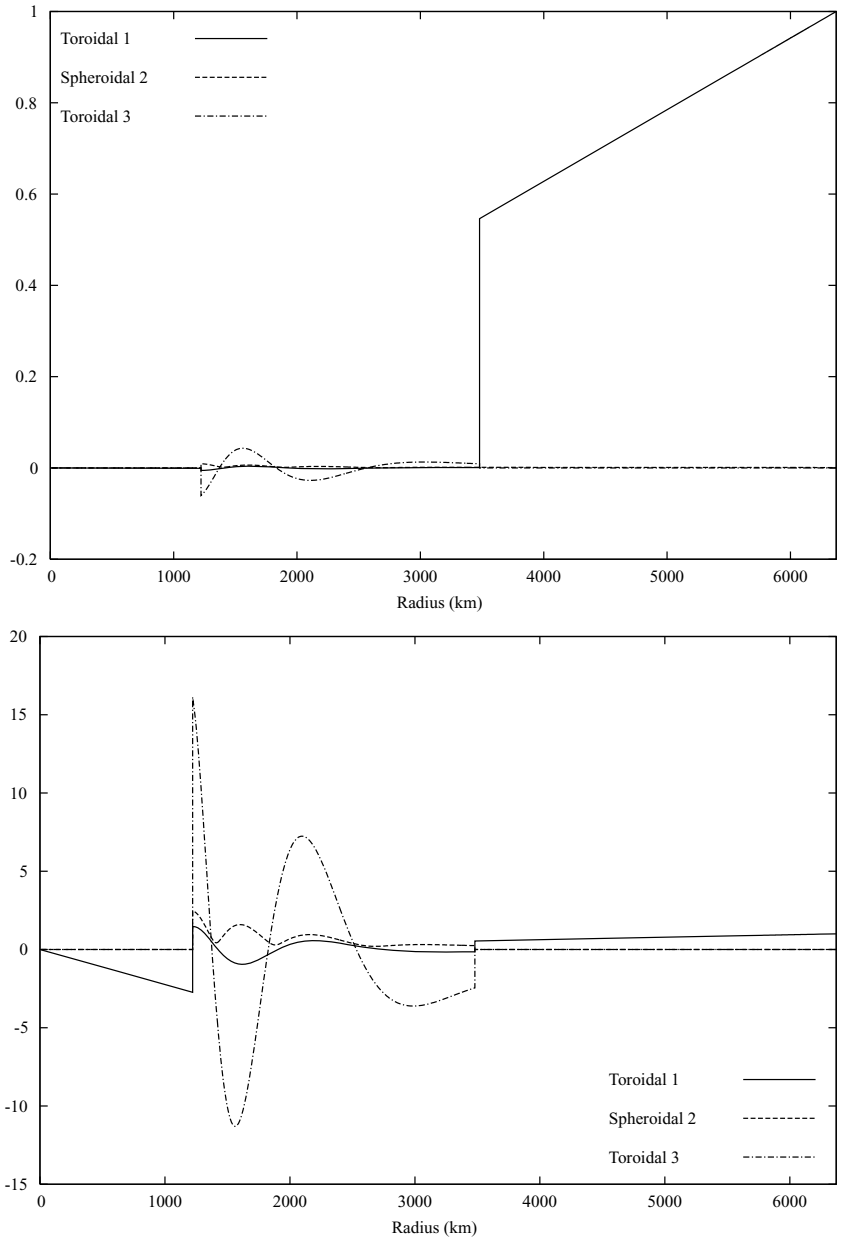

Figure 8. As Fig. 6 for the modes indicated by triangles in the top panel of Fig. 5. $N^2 = -\,1.72 \times 10^{-9}$ rad^2 s^{-2} everywhere in the outer core. The eigenperiods are 405.4 (top panel) and 425.0 solar days (bottom panel). The first mode is dominantly the CW whereas the second mode is a pseudo-mode of the outer core.

must be truncated. This implies that we expect that the amplitudes rapidly decrease as ℓ increases. In the numerical study below, series (20) will be cut off after 2, 3, or 4 terms. We will denote the corresponding sums by TS, TST and TSTS, respectively. The TSTS sum is

$$\mathbf{s} = \boldsymbol{\tau}_1^{\pm 1} + \boldsymbol{\sigma}_2^{\pm 1} + \boldsymbol{\tau}_3^{\pm 1} + \boldsymbol{\sigma}_4^{\pm 1}, \tag{23}$$

which includes $\mathcal{D}_1^{\pm 1}(\theta,\, \varphi)$ as well as the following spherical harmonics:

$$\mathcal{D}_2^{\pm 1}(\theta,\, \varphi) = \pm\frac{\sqrt{6}}{2}\cos\theta\sin\theta e^{\pm i\varphi}, \tag{24}$$

$$\mathcal{D}_3^{\pm 1}(\theta,\, \varphi) = \pm\frac{\sqrt{3}}{4}\sin\theta(5\cos^2\theta - 1)e^{\pm i\varphi}, \tag{25}$$

Table 3. Nutation periods (in sidereal days), in an absolute frame of reference, of the FCN and FICN for four models and three coupling chains.

Mode	Model	TS	TST	TSTS
FCN	Oceanless PREM	−459.3	−459.3	−459.3
	Oceanless PREM ($N^2 = 0$)	−459.3	−459.3	−459.4
	1066 A	−459.3	−459.4	−459.4
	1066 A ($N^2 = 0$)	−459.1	−459.2	−459.2
FICN	Oceanless PREM	470.6	472.9	432.7
	Oceanless PREM ($N^2 = 0$)	470.4	472.7	417.8
	1066 A	511.0	513.6	489.6
	1066 A ($N^2 = 0$)	510.4	513.0	449.7

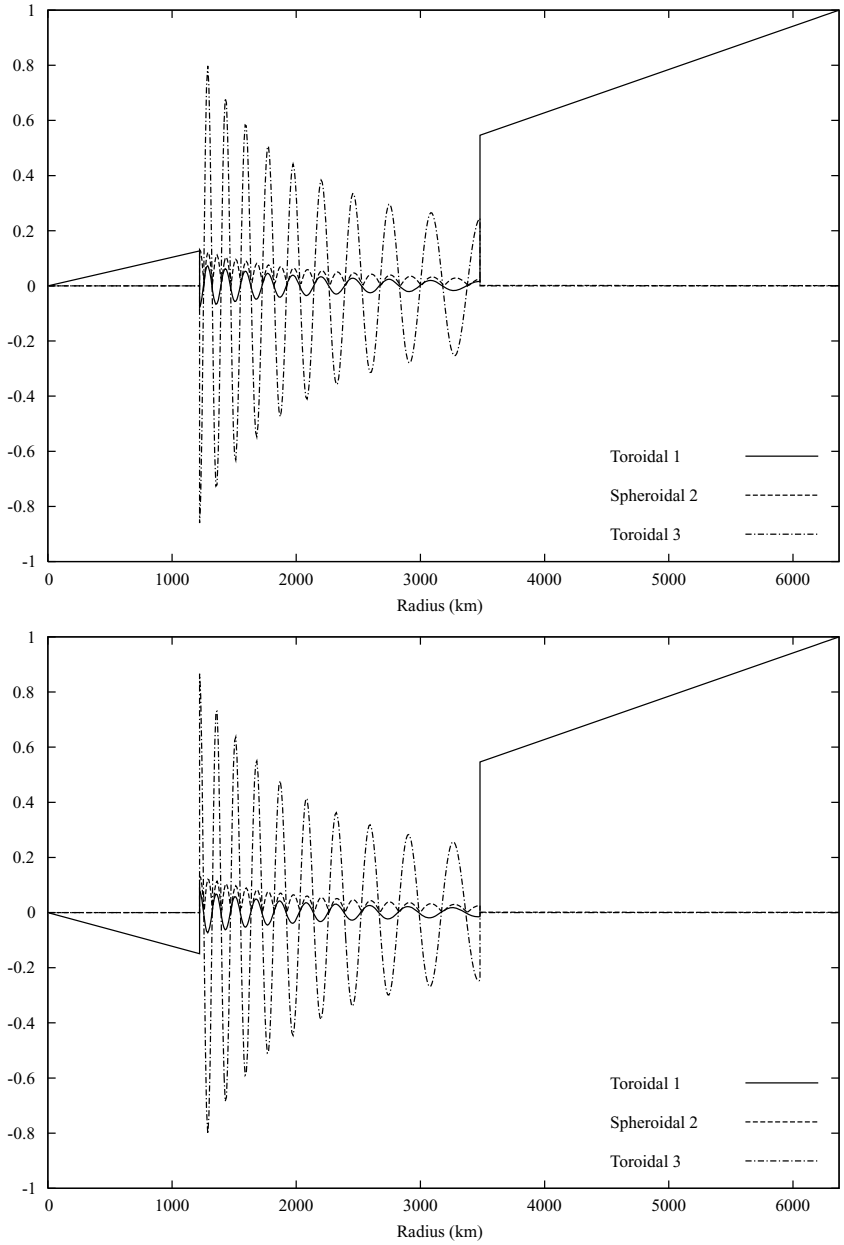

Figure 9. As Fig. 6 for the modes indicated by crosses in the lower panel of Fig. 5. $N^2 = -4.0375 \times 10^{-9}$ rad^2 s^{-2} everywhere in the outer core. The eigenperiods are 403.5 (top panel) and 407.4 solar days (bottom panel). Both modes share a similar wobble of the mantle. The amplitude of the oscillations in the outer core is comparable to the wobble amplitude.

and

$$\mathcal{D}_4^{\pm 1}(\theta,\,\varphi) = \pm\frac{\sqrt{5}}{4}\sin\theta\cos\theta(7\cos^2\theta - 3)e^{\pm i\varphi}. \tag{26}$$

To picture the eigendisplacement **s**, we will integrate $|\mathbf{s}|^2$ over the surface of the unit sphere

$$\int_0^{\pi}\int_0^{2\pi} |\mathbf{s}|^2 \sin\theta \,\mathrm{d}\theta\,\mathrm{d}\varphi = \sum_{\ell=1,\,3,\,5,\,\ldots}^{\infty}\left[\frac{1}{2}\left(W_\ell^{\pm 1}\right)^2 + \left(U_{\ell+1}^{\pm 1}\right)^2 + \frac{1}{2}\left(V_{\ell+1}^{\pm 1}\right)^2\right], \tag{27}$$

normalize the eigenfunctions so that $W_1^{\pm 1}(R) = 1$ at the surface $r = R$, and plot $W_1^{\pm 1}$, $\sqrt{2(U_2^{\pm 1})^2 + (V_2^{\pm 1})^2}$, $W_3^{\pm 1}$, and $\sqrt{2(U_4^{\pm 1})^2 + (V_4^{\pm 1})^2}$ as a function of r.

Many studies, in which it is assumed that the core spectrum contains eigenvalues, showed that the convergence of series (20) of vector spherical harmonics is slow when one tries to compute the hypothetical inertia-gravity modes of an inviscid liquid core (for instance, Johnson & Smylie 1977; Rieutord 1991; Crossley 1993; Wu & Rochester 1993). Therefore, we should not expect that truncated eq. (23) correctly represents inertia-gravity modes of the outer core, if they exist. For that reason, we call the computed modes, 'pseudo-modes'. In the following, we focus on the rotational modes and want to explore the influence of the dynamics of the liquid core.

4 INTERACTION OF ROTATIONAL MODES WITH CORE DYNAMICS

Fig. 1 shows that the nutational modes are embedded into the inertia-gravity spectrum of the liquid core. Therefore, we may wonder how much the eigenfrequency of a rotational mode changes if it is close to the frequency of a planetary mode or pseudo-mode. First, we show that the frequencies of rotational and planetary modes are well separated, so that two modes belonging to different families do not couple. Next, by assuming a uniform N^2 in the liquid core, varying its value and computing in a systematic way the pseudo-modes of the models, we show that they can indeed interact with the nutational modes. Because the liquid core is convecting at a speed of a few meters per year and is therefore well mixed, its stratification is thought to be nearly adiabatic, so that N^2 is close to zero. Variations of a few 10^{-8} rad^2 s^{-2} about zero are allowed by inversion of normal mode data (Masters 1979). We will take $\pm 2 \times 10^{-8}$ rad^2 s^{-2} as upper and lower bounds for the N^2 value. To assume a uniform N^2 may look like an oversimplification. However, as stated above, the truncature of coupling chain (16) makes a more refined treatment of the core structure superfluous. Moreover, a heterogeneous N^2 would pointlessly complicate the pattern of pseudo-modes frequencies.

4.1 Planetary modes

We mentioned in Section 2.2 that the only known regular inertial modes of a non-gravitating and incompressible liquid shell are purely toroidal modes called 'planetary' or 'Rossby' modes. Their eigenfrequencies are given by

$$\omega_m = \frac{2\Omega}{m+1}, \tag{28}$$

with $m > 0$, and the only non null toroidal scalar is

$$W_m^m = Ar^m, \tag{29}$$

where A is a constant determined by the initial conditions (Rieutord & Valdaretto 1997). The motion is accompanied by a pressure variation of degree $m + 1$ that behaves like r^{m+1}. The case $m = 1$ is the tilt-over mode that is actually a mode of the whole Earth. Viewed from inertial space, it is a steady and rigid rotation of the body at the speed Ω about an axis that is slightly inclined with respect to the z-axis of the rotating reference frame. Since it does not depend on the structure and shape of the body, it serves as a useful test for the correctness of the theory and accuracy of the computation (Rogister 2001; Rogister & Rochester 2004). When $m \neq 1$, the

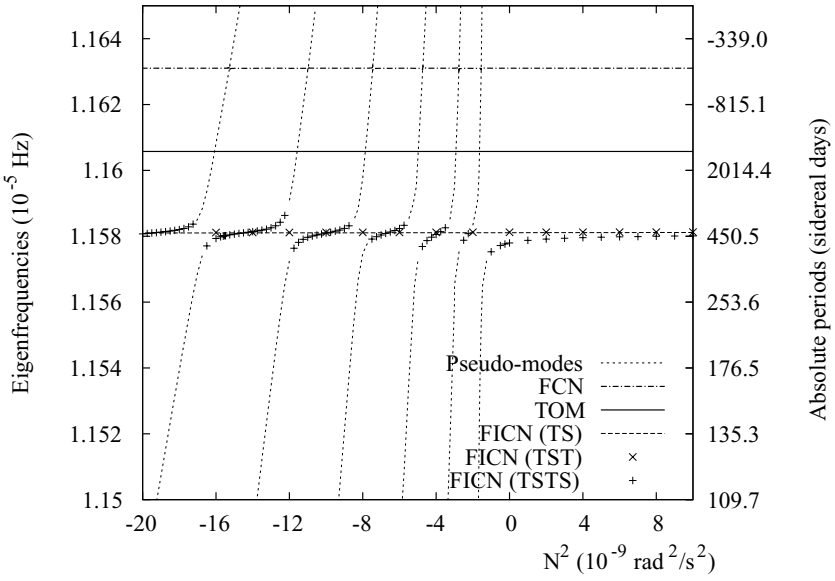

Figure 10. Eigenfrequencies of the tilt-over mode (TOM, the nutation period of which is exactly 1 sidereal day), FCN and FICN for the TS, TST and TSTS coupling chains, and eigenfrequencies of pseudo-modes for the TSTS coupling chain as a function of the uniform squared Brunt–Väisälä frequency in the outer core. Pseudo-modes along a branch are such that V_2^1, W_3^1 and V_4^1 have the same number of nodes in the outer core. No pseudo-mode was found in that frequency range for the TS and TST coupling chains. The nutation period is the period in an absolute frame of reference.

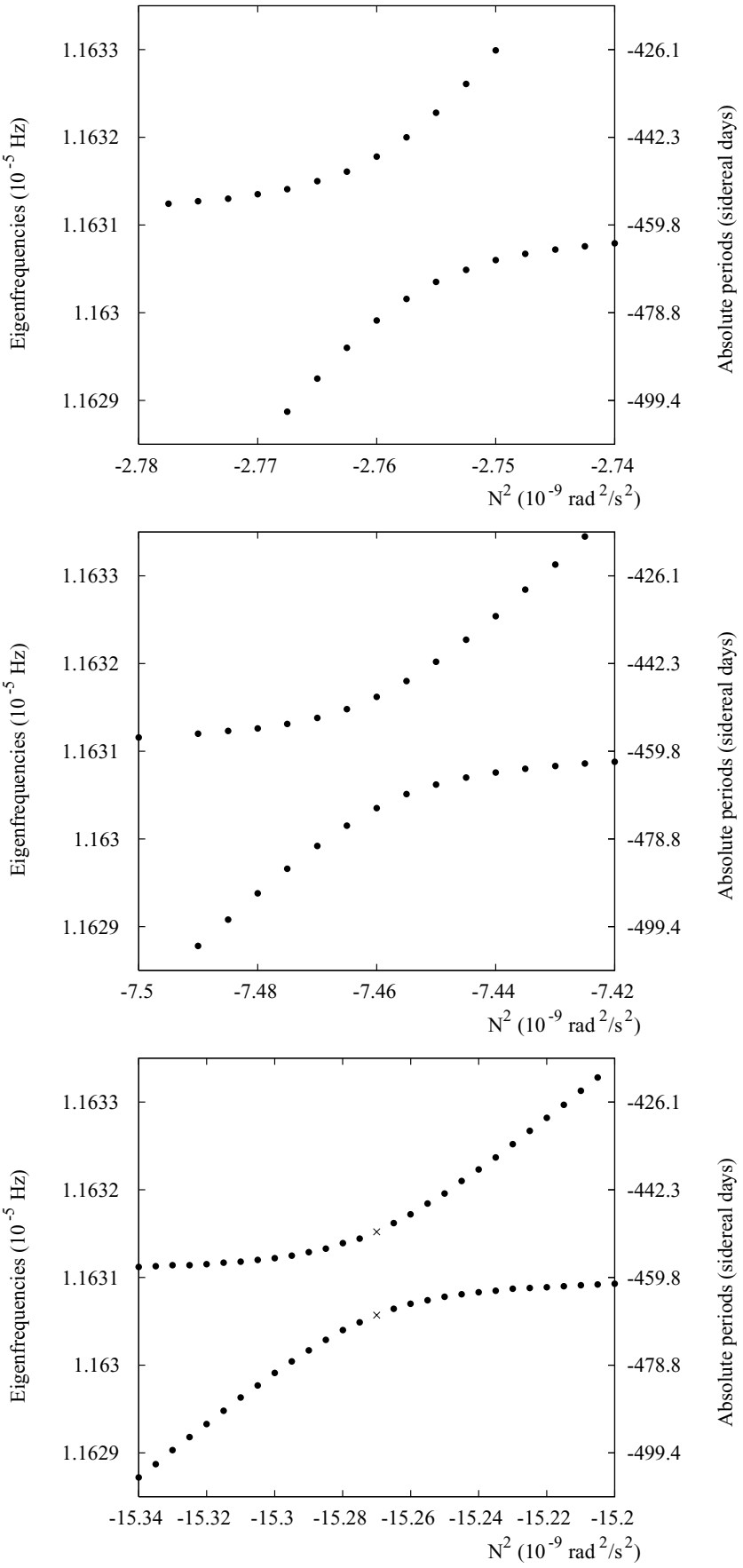

Figure 11. Zooms in on the avoided crossings between the FCN branch and second (top panel), fourth (middle panel) and sixth (bottom panel) pseudo-modes branches of Fig. 10. The eigenfunctions of the modes indicated by crosses are shown in Fig. 12.

frequencies (28) and displacements (29) are not exact solutions for the modes of a gravitating and compressible liquid core. Fig. 2 shows the periods of planetary modes of PREM and the corresponding periods, given by $2\pi/\omega_m$, of a non-gravitating and incompressible core. There is a small difference between the two sets of eigenperiods because, in the gravitating and compressible core, the eigendisplacements are not pure toroidal modes. The toroidal displacement $\boldsymbol{\tau}_m^m$ couples with the spheroidal and toroidal displacements of harmonic degrees $l > m$ according to eq. (16), which involves gravity variations. Generally, the eigenfrequencies computed for both the TST and TSTS coupling chains agree to within 10^{-5} per cent and the spheroidal displacement of degree $m + 3$ is approximately 10 times smaller than the spheroidal displacement of degree $m + 1$. Although it is satisfying that our numerical code provides the planetary modes, they are of limited interest in this study because their frequencies are too different from those of the nutational modes to influence them.

We now consider the rotational modes, first the CW, then we turn to the FCN and FICN.

4.2 Chandler wobble

A first account of the influence of the core dynamics on the CW was given by Rogister & Valette (2005). We provide here more details.

First, in order to avoid the complications due to the oceans, we consider an oceanless earth model by replacing the global ocean of

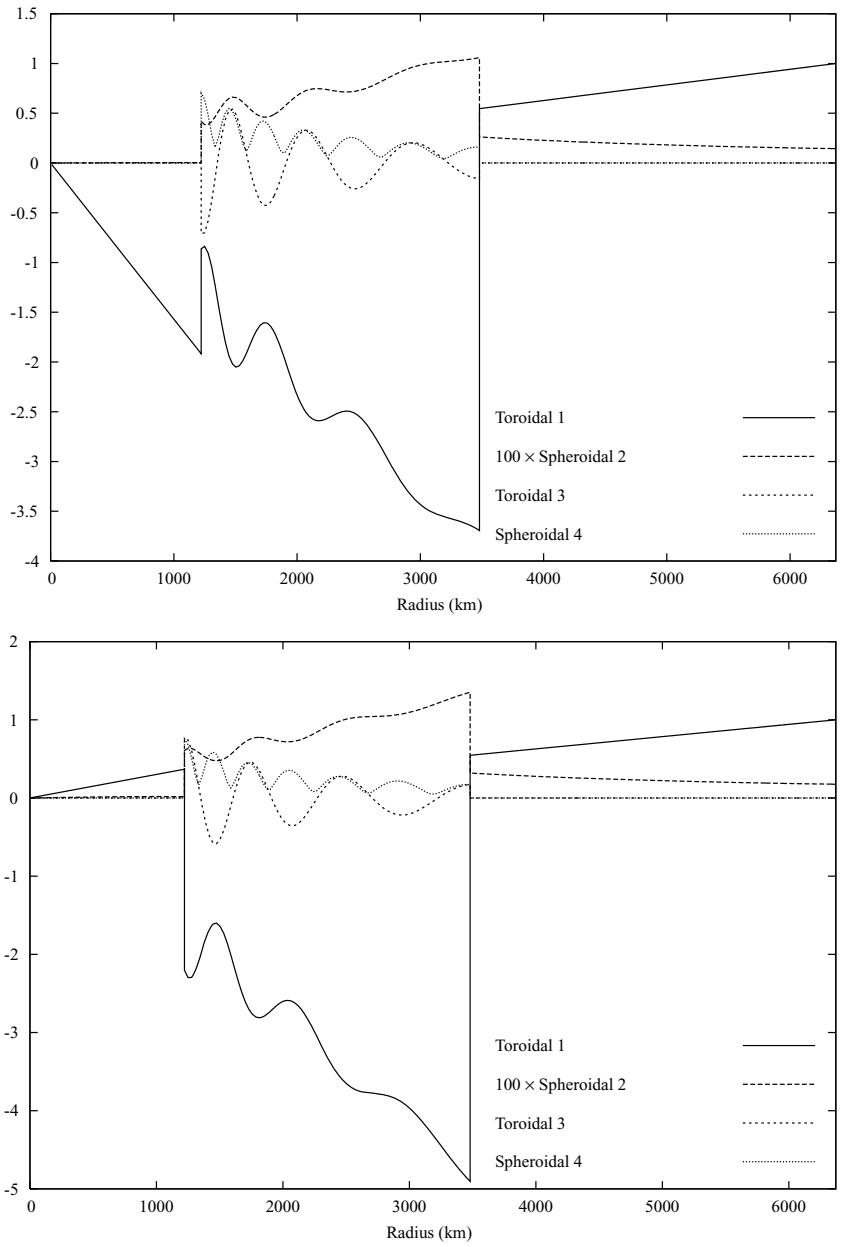

Figure 12. Eigenfunctions of the modes indicated by crosses in Fig. 11 for $N^2 = -15.27 \times 10^{-9}$ rad^2 s^{-2}. The nutation periods are -450.5 (top panel) and -467.7 (bottom panel) sidereal days. The spheroidal displacements of degrees 2 and 4 are shown as $100 \times \sqrt{2(U_2^1)^2 + (V_2^1)^2}$ and $\sqrt{2(U_4^1)^2 + (V_4^1)^2}$, respectively. The degree-1 toroidal displacement in the liquid core is the superposition of a linear function associated to the FCN and oscillations associated to the pseudo-mode. It is to be compared with Figs 2 and 3 of Rogister (2001) that show the FCN eigenfunction without the influence of pseudo-modes. The changes of the signs of the eigendisplacements are the same as for the avoided crossings between the Chandler wobble and pseudo-modes.

the PREM (Dziewonski & Anderson 1981) by a solid crust. The density, wave velocities and quality factors of our model are given in Table 1.

Table 2 shows the CW period for the modified PREM and 1066 A (Gilbert & Dziewonski 1975) for the TS, TST and TSTS coupling chains. As an illustration, Fig. 3 displays the eigenfunctions for the oceanless PREM and the TST coupling chain. As expected, the dominant displacement is a wobble of the mantle alone. In the mantle, U_2^{-1} and V_2^{-1} are roughly 10^3 smaller than W_1^{-1} and U_4^{-1}, V_4^{-1} and W_3^{-1} are approximately 10^6 to 10^7 smaller than W_1^{-1}. In the inner core, W_1^{-1} is from 300 to 10 000 times bigger than the other scalars. The amplitudes of the tangential displacements in the outer core are roughly 50 times bigger than the radial displacements.

Second, we modify the N^2 profile to make it constant throughout the liquid core. For a given N^2 profile, that is for a given earth model, we compute the CW and pseudo-modes eigenfrequencies in the range 20–40 nHz. By varying N^2, we then plot the eigenfrequencies as a function of N^2 for the TS and TST coupling chains. In Fig. 4, the dashed line is the CW branch and the solid lines are pseudo-modes branches. Along a pseudo-modes branch, the displacement scalars have a constant number of nodes in the outer core. For instance, along the first branch on the right, the toroidal scalar W_1^{-1} has 1 node in the outer core. The number of its nodes increases by 1 as one moves to the next branch to the left.

We are interested in the vicinity of the points where the pseudo-modes and CW branches seem to cross. Actually, if we look closer, we see that all the crossings are avoided. To exemplify the avoided crossings, we consider the third and19th branches of the TST coupling.

The top panel of Fig. 5 shows the avoided crossing between the third pseudo-modes and Chandler branches, where $N^2 \in [-1.82, -1.72]\ \ 10^{-9}$ rad^2 s^{-2}. On both the right and left ends of the plot, the difference between two eigenperiods of a same model is about 15–20 d. As shown in Fig. 6 for the modes marked by + signs in Fig. 5, the motions are either a dominant wobble of the mantle, that is, the CW, or an oscillation of the liquid outer core. As N^2 increases, the eigenfrequencies are getting closer but are always separated by a few days. When the difference between their frequencies is the smallest, both modes share similar eigendisplacements, namely a wobble of the mantle and oscillations in the outer core of the same amplitude as the wobble, as Fig. 7 shows for the displacements of the modes designated by crosses in Fig. 5. Thus, we have a double CW with two periods separated by 2.5 solar days. As N^2 still increases, the separation between the eigenfrequencies now increases. Fig. 8 shows the eigendisplacements for the modes designated by triangles in Fig. 5. We have two different modes: the mode with the shortest period is dominantly a wobble of the mantle, while the other one is dominantly a pseudo-mode of the liquid core. The difference between their periods is approximately 20 d.

It is noticeable that, for the modes plotted in Figs 6–8, the signs of the scalars W_1^{-1} and W_3^{-1} in the inner and outer cores are opposite in the top and bottom panels. Although we do not show U_2^{-1} and V_2^{-1} separately, we have checked that it is also true for them. By going through the avoided crossing, the pseudo-mode of the outer core shown in the top panel of Fig. 6 becomes the pseudo-mode in the bottom panel of Fig. 8. The only difference between the eigendisplacements is a change of sign for W_1^{-1}, U_2^{-1}, V_2^{-1} and W_3^{-1} in the inner and outer cores. In Fig. 7, making half the sum (resp. difference) of the eigendisplacements of both panels gives a pure CW (resp. pseudo-mode).

The avoided crossing between the 19th pseudo-modes and Chandler branches is illustrated in the bottom panel of Fig. 5. The eigenfunctions of the modes designated by crosses, for the model having $N^2 = -4.0375 \times 10^{-9}$ rad^2 s^{-2} in the outer core, are shown in Fig. 9. Again, we obtain a double CW. The separation between the two periods is about 3.9 solar days. The interaction is thus stronger than the interaction between the third branch and the Chandler branch but the signs of the displacement scalars follow the same rules: they are, for the two modes, of different signs in the inner and outer cores and the eigenfunctions of the modes are mixed in such a way that, along a branch, the signs of the scalars in the inner and outer cores change across the avoided crossing.

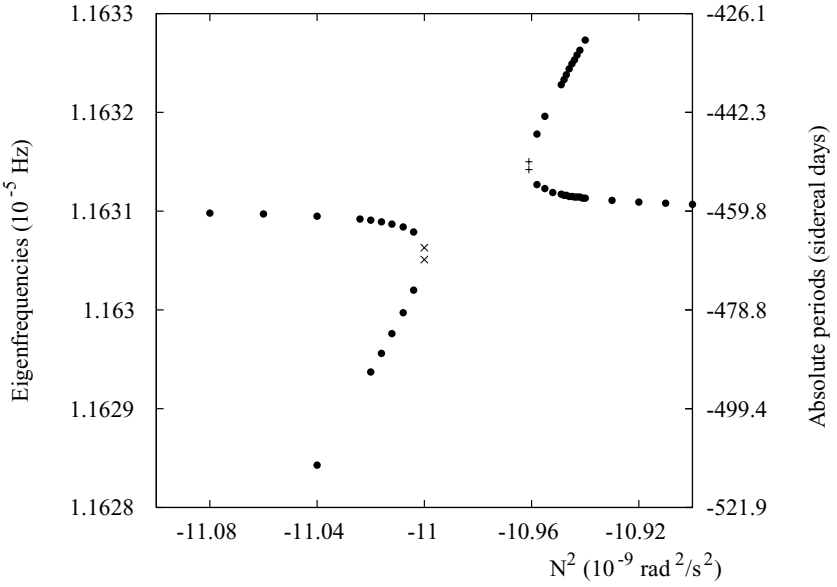

Figure 13. Zoom in on the intersection between the FCN (horizontal) and fifth pseudo-modes (inclined) branches of Fig. 10. In the range $N^2 \in [-11.00, -10.96]\ 10^{-9}$ rad^2 s^{-2}, where the two branches merge, the eigenfrequency is complex. Since our numerical code is not meant to compute complex eigenvalues, we cannot plot the real part of the eigenfrequency in that range. The eigendisplacements of the modes indicated by crosses are shown in Fig. 14, those of the modes indicated by + signs are shown in Fig. 15.

Avoided crossings can be found in many branches of physics. For instance, they occur in quantum systems that depend on a certain number of parameters when, by varying a parameter, two eigenvalues of a Hamilton operator come close to each other (Landau & Lifshitz 1977). Various types of avoided crossings in quantum systems were described by Rotter (2001). The eigenfrequencies of gravity and capillary waves at the surface of a fluid also show avoided crossings when, for example, the finite amplitude of the waves is taken as a parameter (MacKay & Saffman 1986). Avoided crossings are common in the astrophysical literature. In a seismological context, the non-crossings of families of seismological modes in a dispersion diagram that shows the eigenfrequencies as a function of harmonic degree ℓ are also referred to as 'avoided crossings' (Dahlen & Tromp 1998, pp. 303–305).

The conclusion of this subsection is that the dynamics of the outer core influences the CW through avoided crossings that, in narrow N^2 ranges, allow for the existence of a double CW, the periods of the two wobbles being separated by a few days.

4.3 Free core nutation and free inner core nutation

The periods of the FCN and FICN for 1066 A and our oceanless version of PREM are given in Table 3. The FICN period is more sensitive than that of the FCN to the length of the coupling chain. We cannot even conclude that a TSTS chain is sufficient to compute accurately the FICN period, which changes by 5–8 per cent when one adds one term to the TST chain to obtain the TSTS chain. The

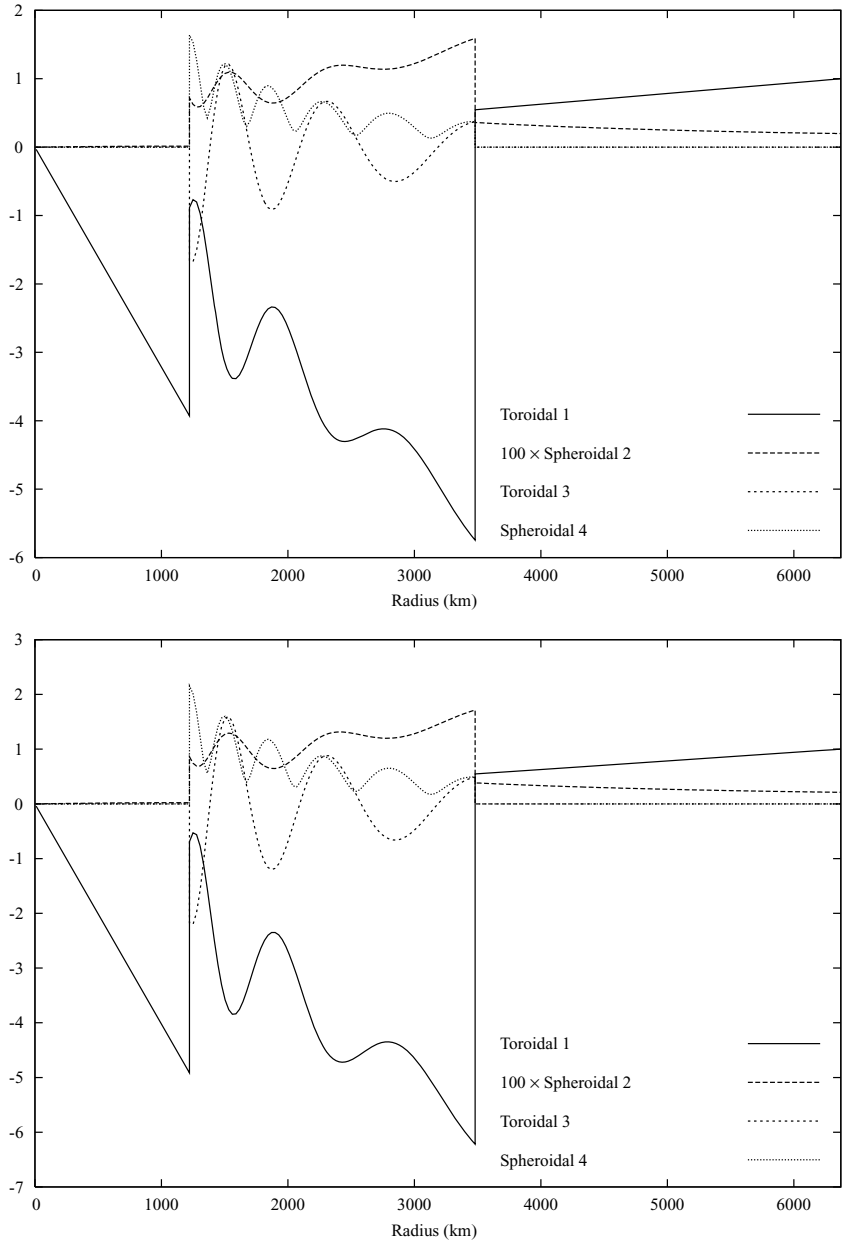

Figure 14. Eigenfunctions of the modes indicated by crosses in Fig. 13 for $N^2 = -11 \times 10^{-9}$ rad^2 s^{-2}. The nutation periods are -466.7 (top panel) and -468.9 (bottom panel) sidereal days. The eigenfunctions are almost the same since they continuously vary along the FCN and pseudo-modes branches that merge.

FCN and FICN eigendisplacements for the oceanless PREM and TST chain were shown by Rogister (2001).

We numerically investigate the spectrum of a rotating earth model in the nearly diurnal band for coupling chains having $m = 1$, which includes both the FCN and FICN, by varying the N^2 parameter in the liquid core of our oceanless PREM. In Fig. 10, we plot the eigenfrequencies found between 1.15×10^{-5} and 1.165×10^{-5} Hz, corresponding to relative periods of approximately 86956.5 and 85836.9 s, respectively, in a corotating frame. The nutation period T_a shown on the right ordinate axis is the period in an absolute reference frame. It is related to the relative period T_r in a corotating frame by

$$T_a = \frac{T_r}{T_r/T - 1}, \tag{30}$$

where $T = 1$ sidereal day = 86164.1 s. Of course, the relative period of the tilt-over mode is always one sidereal day. The nutation period of the FCN is approximately -459 sidereal days. Pseudo-modes cannot be found in the frequency range [1.15, 1.165] 10^{-5} Hz for either the TS and TST chains. When the FCN and FICN do not interact with pseudo-modes, their frequencies are not sensitive to the Brunt–Väisälä frequency. But, the TSTS chain contains pseudo-modes in that frequency range. In the following, we explore the crossings between pseudo-modes branches and, first, the FCN branch and, second, the FICN branch.

4.3.1 Free core nutation

To explain the discrepancy between the nutation period of the FCN determined from gravity measurements or VLBI data, which

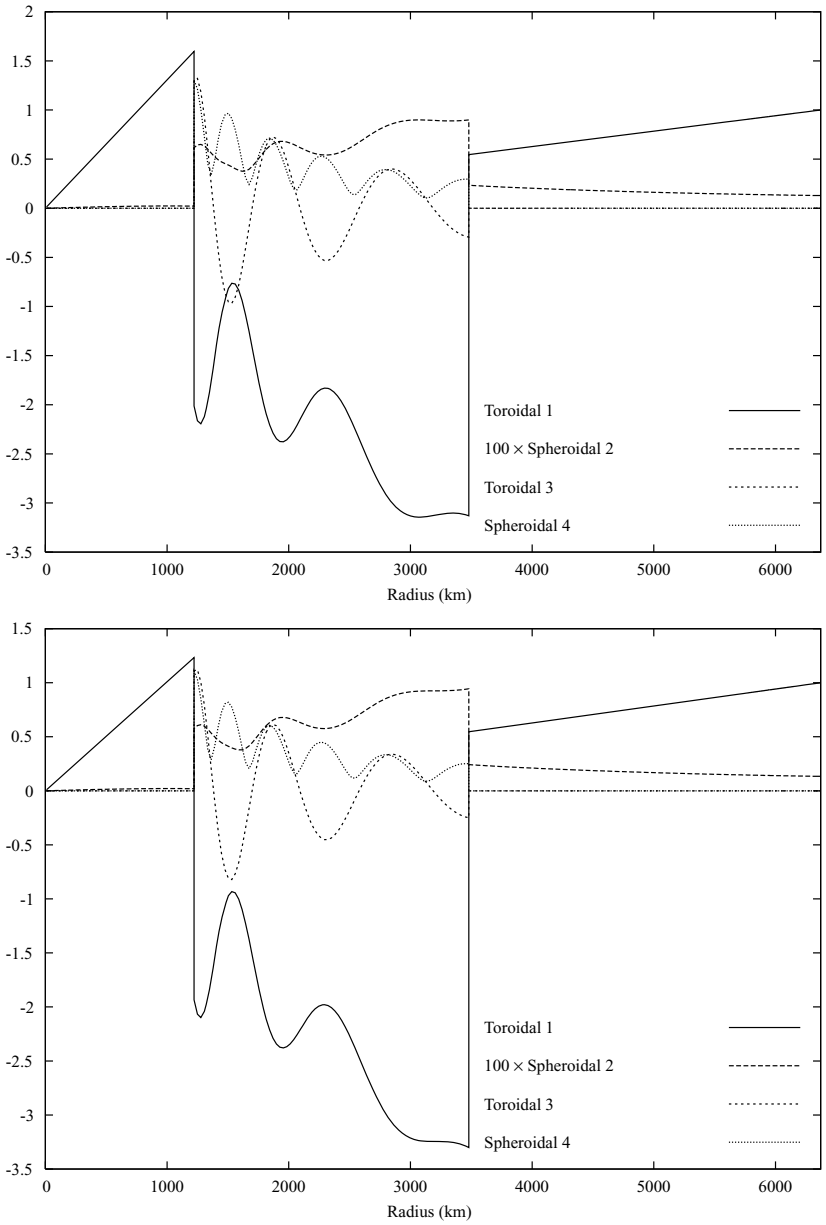

Figure 15. Eigenfunctions of the modes indicated by + signs in Fig. 13 for $N^2 = -10.96 \times 10^{-9}$ rad^2 s^{-2}. The nutation periods are -450.9 (top panel) and -452.4 (bottom panel) sidereal days. The signs of the displacement scalars in the inner and outer cores are opposite to those of the scalars shown in Fig. 14, except for W_1^1 in the outer core. But, the oscillations of W_1^1 around the straight line that represents the nutation of the outer core is opposite in this figure and Fig. 14.

is approximately −429 d (Florsch & Hinderer 2000; Hinderer *et al.* 2000; Mathews *et al.* 2002), and its theoretical period, approximately −459 d, Gwinn *et al.* (1986) or Lumb & Aldridge (1991) suggested that a gravity-inertial mode with a period close to the FCN period would change the latter. Before we explore this idea, we mention that the 30-d discrepancy is commonly attributed to a departure of the actual dynamical flattening of the CMB from its hydrostatic value (Gwinn *et al.* 1986).

A first look at Fig. 10 already convinces us that the interaction of the pseudo-modes branches with the FCN branch is weaker than that with the FICN branch. A closer inspection of the interaction between the FCN branch and the second, fourth and sixth pseudo-modes branches reveals that the crossings are avoided (Fig. 11). Moreover, contrary to the CW, the spacing between the closest eigenfrequencies in an avoided crossing decreases as the number of nodes of the eigenfunctions in the outer core increases, that is when N^2 decreases. For the three avoided crossings shown in Fig. 11, the closest eigenperiods are −442.3 and −475.7, −448.8 and −472.0, and −450.5 and −467.7 sidereal days for, respectively, $N^2 = -2.7575 \times 10^{-9}$, -7.46×10^{-9} and -15.27×10^{-9} rad^2 s^{-2}. The eigendisplacements corresponding to the eigenperiods of −450.5 and −467.7 d, which are indicated by crosses in Fig. 11, are shown in Fig. 12. They can be compared with the eigendisplacements of the FCN shown in Figs 2 and 3 of Rogister (2001) for the TST coupling chain. The spheroidal scalars U_2^1 and V_2^1 are of the same order of magnitude for both the TST and TSTS coupling chains. On the contrary, because of the presence of a pseudo-mode, the toroidal scalar W_3^1 is two orders of magnitude bigger for the TSTS coupling chain than for the TST coupling chain. In Fig. 12, the W_1^1 scalar in the outer core is the superposition of a rigid nutation associated to the FCN and oscillations associated to a pseudo-mode. The signs of the eigendisplacements and their changes across an avoided crossing follow the same rules as those described for the avoided crossings between the CW and pseudo-modes.

By zooming in on the crossings between the FCN branch and the first, third and fifth pseudo-mode branches in Fig. 10, we find another kind of interaction, which is illustrated in Fig. 13 for the fifth pseudo-mode and FCN branches. The horizontal (FCN) and inclined (pseudo-mode) branches merge at the two exceptional points of approximate abscissa $N^2 = -11.00 \times 10^{-9}$ and -10.96×10^{-9} rad^2 s^{-2}. The frequency of the resulting normal mode becomes complex. However, since our numerical code is not meant to compute complex eigenfrequencies, we cannot plot their real part in Fig. 13, leaving an artificial gap between $N^2 = -11.00 \times 10^{-9}$ and -10.96×10^{-9} rad^2 s^{-2}. By studying the stability of water waves with respect to the variation of a parameter, for example the steepness of the waves, MacKay & Saffman (1986) found similar crossings of the complex eigenvalues (in particular, see their Fig. 4, which is a plot of the complex eigenfrequency as a function of the wave amplitude). Because the waves then become unstable, the crossings are called 'bubbles of instability'. Similar crossings were also obtained by Gubbins & Gibbons (2002) for dynamo waves and by Stefani *et al.* (2006) for a simple kinematic α^2 dynamo. They found that, by varying certain parameters, for instance the magnetic Reynolds number or the helical turbulence, two purely imaginary eigenvalues, which correspond to steady decaying or growing magnetic fields, coalesce to form a complex conjugate pair of oscillatory modes. This phenomenon, which is actually the opposite of a bubble of instability, provides a plausible mechanism for the reversal of the magnetic field. A mathematical description of such exceptional points can be found in (Kato 1976, pp. 65–66).

The eigendisplacements of the modes indicated by crosses in Fig. 13, close to the essential point where the eigenfrequencies coalesce, are shown in Fig. 14. They are, of course, almost identical. By comparing with the eigendisplacements, shown in Fig. 15, of the modes indicated by + signs in Fig. 13, we see that W_3^1 changes its sign across the crossing, as does W_1^1 in the inner core. We have checked that the signs of U_2^1, V_2^1, U_4^1 and V_4^1 also change from Figs 14 and 15. In the outer core, W_1^1 has the same sign for the four modes displayed in both Figs 14 and 15 but its oscillations are opposite in Figs 14 and 15.

Although this kind of interaction between the FCN and pseudo-modes looks interesting, it cannot be a real feature of the dynamical system. It is an artefact due to the truncation of the coupling chain (20). Indeed, the FCN frequency cannot leave the real axis and become complex, as Fig. 1 shows.

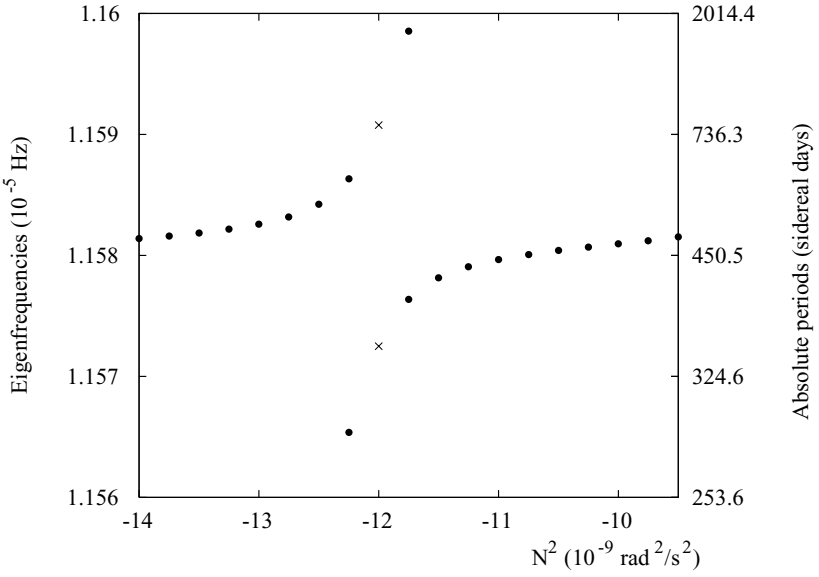

Figure 16. Zoom in on the avoided crossing between the FICN and fifth pseudo-modes branch in Fig. 10. As for the CW, the influence of the outer core dynamics on the FICN always results in avoided crossings. The eigenfunctions of the modes indicated by crosses are shown in Fig. 17.

The coupling of pseudo-modes and FCN through avoided crossings, albeit very weak and occurring for narrow N^2 ranges, is a plausible candidate to bring the theoretical period of the FCN closer to the period deduced from the resonance with the observed forced nutations, in particular the retrograde annual nutation. 'Retrograde' here refers to an absolute system of reference. Our results indeed indicate that the theoretical FCN period closest to −429 d, which is the 'observed' period, is −442.3 sidereal days. Moreover, since the avoided crossings actually generate a double FCN, the second FCN would also modify the amplitude of the observed retrograde annual nutation, maybe reducing the need for other geophysical explanations to fill the gap between the 'observed' period of −429 d and the period of −459 d for PREM.

4.3.2 Free inner core nutation

We have mentioned at the beginning of Section 4.3 that 4 terms in the coupling chain (16) may not be enough to estimate accurately the period of the FICN. Moreover, the theoretical FICN period for PREM or 1066 A, roughly ranging from 433 to 514 d (Table 3), is still very far from the period that is estimated from the observed amplitudes of the forced nutations, which are determined by using VLBI data, and that is 1038 ± 105 sidereal days (Mathews *et al.* 2002). According to them, the discrepancy comes from the effect of the electromagnetic coupling between the inner and outer cores, which is neglected here.

As for the FCN, we aim at verifying that the dynamics of the outer core can significantly alter the FICN frequency. Fig. 10 shows

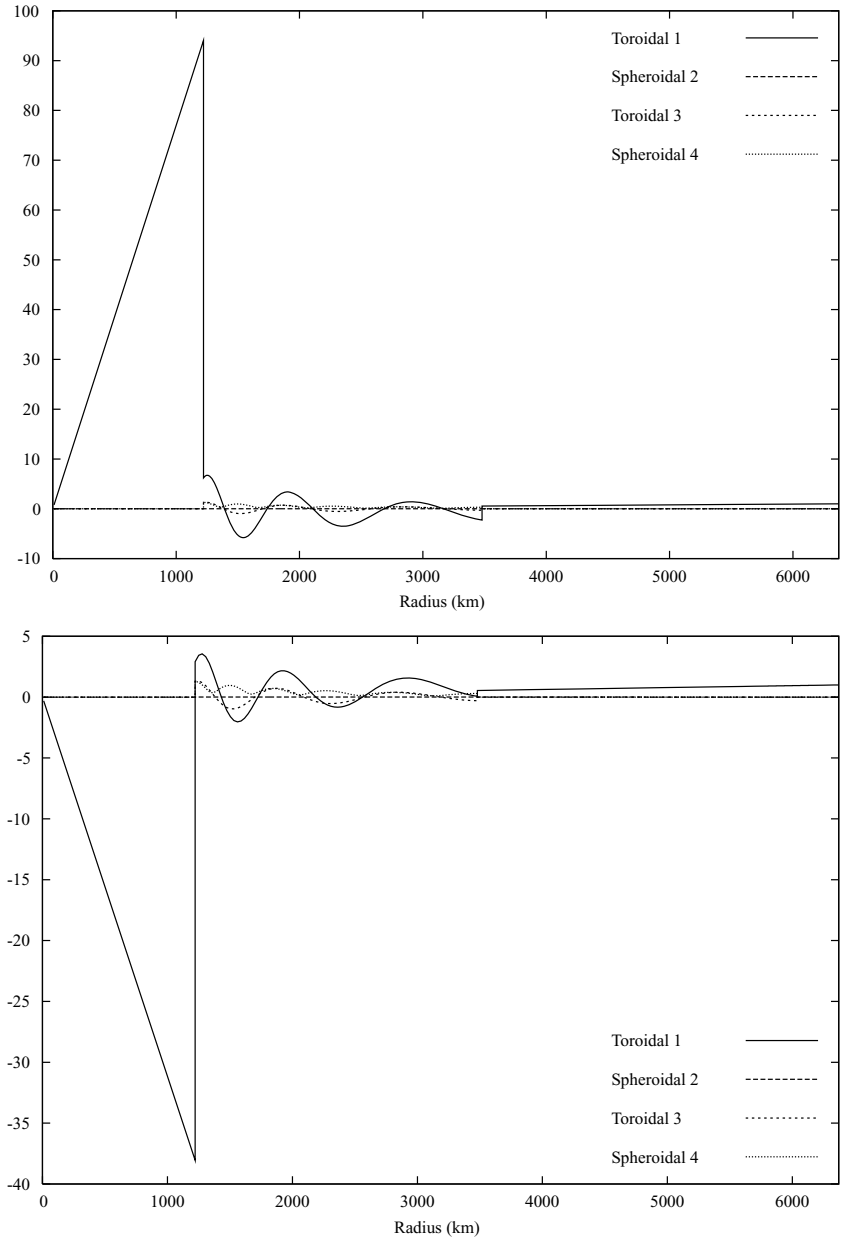

Figure 17. Eigenfunctions of the modes indicated by crosses in Fig. 16 for $N^2 = -12 \times 10^{-9}$ rad^2 s^{-2}. The nutation periods are 348.9 (top panel) and 774.3 (bottom panel) sidereal days. The total displacement field is dominated by the nutation of the inner core.

that the FICN is strongly influenced by the pseudo-modes, as can be intuitively expected. We find that the interaction between the FICN and the pseudo-modes always gives rise to avoided crossings, an example of which is shown in Fig. 16. The eigendisplacements of the modes indicated by crosses in Fig. 16 are plotted in Fig. 17. For the mode in the top (resp. bottom) panel, the eigenperiod is 348.9 (resp. 774.3) sidereal days. The displacement field is dominated by the nutation of the inner core. The amplitude of the oscillation in the outer core is an order of magnitude smaller than the amplitude of the nutation of the inner core, in contrast to the avoided crossings for the CW and FCN where the eigenfunctions of the modes mixed with equal amplitudes. The displacement in the mantle is mainly a rigid nutation, the angle of which is about 200 to 500 times smaller than the nutation angle of the inner core, the normalization of the eigendisplacements is such that $W_1^1 = 1$ m at the surface. Further numerical computation of the modes near the avoided crossings reveals that their eigenfunctions exhibit a large nutational component in the inner core. Roughly, the period of such modes ranges from 200 to 1000 d. Consequently, it might be in agreement with the value deduced by Mathews *et al.* (2002) from the observation of the forced nutations. Nevertheless, rather than being a definite explanation for the 'observed' period of the FICN, this is a motivation to improve the accuracy of the calculation of the FICN and the knowledge of the core dynamics of realistic earth models.

To end this subsection, we mention that avoided crossings associated to strong coupling between modes are frequently encountered in the astrophysics literature. For instance, Aizenman *et al.* (1977) described the avoided crossings between acoustic, gravity and fundamental modes occurring during the evolutionary sequence of a star. Hasan & Christensen-Dalsgaard. (1992) described the avoided crossings between acoustic, gravity, Lamb and magnetic modes in an isothermal stratified atmosphere in the presence of a uniform vertical magnetic field. Namely, they derive analytical formulae for the minimum separation between two modes in an avoided crossing in a weak-field and low-frequency approximation.

5 DISCUSSION AND CONCLUSIONS

An alternative theoretical approach to the computation of the nutational modes consists in solving the equations of conservation of angular momentum, or Liouville's equations, which are obtained by integrating over the inner core, outer core and entire Earth the cross product of the position vector $\mathbf{r}$ and the local equations of motion. Initiated by Hough (1895) and Poincaré (1910) who considered a liquid core contained in a rigid mantle, the method was extended by Molodensky (1961) and Sasao *et al.* (1980) to take the elasticity of the mantle into account, and later by Mathews *et al.* (1991) and de Vries & Wahr (1991) to include a solid elastic inner core. The approximation for the displacement field is a TS coupling chain where the toroidal term $\boldsymbol{\tau}_1^{\pm 1}$ is supposed to be a linear function of the radius that is discontinuous at the ICB and CMB. Moreover, the spheroidal term $\boldsymbol{\sigma}_2^{\pm 1}$ is computed for a non-rotating spherical model perturbed by a static body force that is the variation of the centrifugal force induced by the rigid rotation about an equatorial axis given by $\boldsymbol{\tau}_1^{\pm 1}$. Buffett *et al.* (1993) brought improvement by including the effects of the ellipticity and inertia forces on $\boldsymbol{\sigma}_2^{\pm 1}$. Up to now, the studies based on the angular momentum approach have dealt with the free and forced nutations only. However, in view of our coming conclusions, they are not accurate enough to represent the FICN, or possibly the ICW. They should be extended to accommodate for a more complicated flow in the outer core. But, the angular momentum approach is not suited to the study of the interaction between the nutational modes and the inertia-gravity spectrum of the core.

We would like to restate that the approximation that consists in keeping only four terms in coupling chain (20) does not allow for a quantitative interpretation of our results. For instance, we do not claim that they provide constraints on the N^2 parameter, that is, the thermal stratification, in the outer core. We rather want to show that the dynamics of the Earth is possibly richer than often thought or assumed.

Our first conclusion is that the calculation of the free wobbles of the inner core requires more than two terms in the eigendisplacement (20). Our second and main conclusion is that the nutational modes interact with the inertia-gravity modes that we numerically obtained and called 'pseudo-modes'. The frequencies of the pseudo-modes depend on both the speed of rotation and squared Brunt–Väisälä frequency N^2. For narrow ranges of N^2, avoided crossings occur between the frequencies of the pseudo-modes and those of the CW, FCN and FICN. The eigenfunctions of two modes having nearby frequencies are a combination of the eigenfunctions of two isolated modes, one being a rotational mode, the other, a pseudo-mode. The eigenfunctions are mixed with equal amplitudes for the CW and FCN. For the FICN, the amplitude of the nutation of the inner core is an order of magnitude bigger than the oscillations in the liquid core. In avoided crossings, the wobble period of the CW and nutation period of the FCN are shifted by, say, 3–15 d, whereas the nutation period of the FICN is shifted by a few hundred days. Although our conclusions are qualitative, they could provide an alternative explanation, at least partial, to the discrepancies between the predicted and observed frequencies of the nutational modes. In particular, the double or multiple nature of the Chandler frequencies finds here a plausible explanation.

Another approach to the interaction between the nutations and dynamics of the core could be a spectral approach in the time domain that takes the stratification of the core into account, as described by Chaljub & Valette (2004) and Chaljub *et al.* (2007).

Finally, we mention that including viscosity in the fluid core will make its spectrum discrete, except for the zero complex frequency. Series (15) and (16) will then surely be convergent. The interaction of the inertia-gravity modes of a viscous fluid core with the rotational modes is certainly worth exploring, especially as a function of the viscosity.

ACKNOWLEDGMENTS

We gratefully acknowledge financial support from the CNRS-INSU programs DyETI and SEDIT. We thank Michel Rieutord for a helpful discussion on core modes.

REFERENCES

Aizenman, M., Smeyers, P. & Weigert, A., 1977. Avoided crossing of modes of non-radial stellar oscillations, *Astron. Astrophys.,* **58,** 41–46.

Aldridge, K., 1975. Inertial waves and the Earth's outer core, *Geophys. J. R. astr. Soc.,* **42,** 337–345.

Birch, F., 1952. Elasticity and constitution of the Earth's interior, *J. geophys. Res.,* **57,** 227–286.

Blum, P.A., Hatzfeld, D. & Wittlinger, G., 1973. Résultats expérimentaux sur la fréquence de résonance due à l'effet dynamique du noyau liquide, *C. R. Acad. Sci. Paris,* **277,** Sér. B, 241–244.

Buffett, B.A., Mathews, P.M., Herring, T.A. & Shapiro, I.I., 1993. Forced nutations of the Earth: contributions from the effects of ellipticity and rotation on the elastic deformations, *J. geophys. Res.,* **98**(B12), 21 659–21 676.

Bullen, K.E., 1975. *The Earth's Density*, Chapman and Hall, London.
Chaljub, E. & Valette, B., 2004. Spectral element modeling of three dimensional wave propagation in a self-gravitating Earth with an arbitraly stratified outer core, *Geophys. J. Int.,* **158,** 131–144.
Chaljub, E., Komatitsch, D., Vilotte, J.-P., Capdeville, Y., Valette, B. & Festa, G., 2007. Spectral Element Analysis in Seismology, in *Advances in Wave Propagation in Heterogeneous Media*,Vol. 48, Advances in Geophysics, pp. 365–419, eds Wu, R.-S. & Maupin, V., Elsevier, Academic Press, London, UK.
Chandler, S.C., 1891a. On the variation of latitude, *Astron. J.,* **248,** 59–61.
Chandler, S.C., 1891b. On the variation of latitude, *Astron. J.,* **249,** 65–70.
Chandler, S.C., 1901a. On a new component of the polar motion, *Astron. J.,* **490,** 79–80.
Chandler, S.C., 1901b. On a new component of the polar motion, *Astron. J.,* **494,** 109–112.
Crossley, D.J., 1993. The gravity effect of core modes for a rotating Earth, *J. Geomag. Geoelectr.,* **45,** 1371–1381.
Dahlen, F.A. & Tromp, J., 1998. *Theoretical Global Seismology*, Princeton University Press, Princeton, New Jersey.
de Vries, D. & Wahr, J.M., 1991. The effects of the solid inner core and nonhydrostatic structure on the Earth's forced nutations and Earth tides, *J. geophys. Res.,* **96**(B5), 8275–8293.
Dziewonski, A. & Anderson, D., 1981. Preliminary reference Earth model, *Phys. Earth planet. Int.,* **25,** 297–356.
Florsch, N. & Hinderer, J., 2000. Bayesian estimation of the free core nutation parameters from the analysis of precise tidal gravity data, *Phys. Earth planet. Int.,* **117,** 21–35.
Friedman, J.L. & Schutz, B.F., 1978. Secular instability of rotating Newtonian stars, *Astrophys. J.,* **221,** 937–957.
Gilbert, F. & Dziewonski, A.M., 1975. An application of normal mode theory to the retrieval of structural parameters and source mechanisms from seismic spectra, *Phil. Trans. R. Soc.,* **278A,** 187–269.
Greenspan, H.P., 1969. *The Theory of Rotating Fluids*, Cambridge University Press, Cambridge.
Gubbins, D. & Gibbons, S., 2002. Three-dimensional dynamo waves in a sphere, *Geophys. Astrophys. Fluid Dyn.,* **96,** 481–498.
Guo, J.-Y., Greiner-Mai, H. & Ballani, L., 2005a. A spectral search for the inner core wobble in Earth's polar motion, *J. geophys. Res.,* **110,** B10402, doi:10.1029/2004JB003377.
Guo, J.-Y., Greiner-Mai, H., Ballani, L., Jochmann, H. & Shum, C.K., 2005b. On the double-peak spectrum of the Chandler wobble, *J. Geodesy,* **78,** 654–659, doi:10.1007/s00190-004-0431-0.
Gwinn, C.R., Herring, T.A. & Shapiro, I.I., 1986. Geodesy by radio interferometry: studies of the forced nutations of the Earth: 2. Interpretation, *J. geophys. Res.,* **91**(B5), 4755–4765.
Hasan, S.S. & Christensen-Dalsgaard., 1992. The influence of a vertical magnetic field on oscillations in an isothermal stratified atmosphere, *Astrophys. J.,* **396,** 311–332.
Hinderer, J., Boy, J.P., Gegout, P., Defraigne, P., Roosbeek, F. & Dehant, V., 2000. Are the free core nutation parameters variable in time?, *Phys. Earth planet. Int.,* **117,** 37–49.
Hough, S.S., 1895. The oscillations of a rotating ellipsoidal shell containing fluid, *Phil. Trans. R. Soc. Lond. A,* **186,** 469–506.
Hu, X.-G., Liu, L.-T., Ducarme, B., Xu, H.J. & Sun, H.-P., 2007. Estimation of pole tide gravimetric factor at the Chandler period through wavelet filtering, *Geophys. J. Int.,* **169,** 821–829, doi: 101111/j.1365-246X.2007-03330.x.
Huang, C.-L., Dehant, V. & Liao, X.-H., 2004. The explicit scalar equations of inifinitesimal elastic-gravitational motion in the rotating, slightly elliptical fluid outer core of the Earth, *Geophys. J. Int.,* **157,** 831–837.
Jeffreys, H. & Vicente, R.O., 1957. The theory of nutation and the variation of latitude, *Mon. Not. R. astr. Soc.,* **117,** 142–161.
Johnson, I.M. & Smylie, D.E., 1977. A variational approach to whole-Earth dynamics, *Geophys. J. R. astr. Soc.,* **50,** 35–54.
Kato, T., 1984. *Perturbation Theory for Linear Operators, Grundlehren der mathematischen Wissenschaften*, 2nd edn,Vol. 132, Springer-Verlag, Berlin.
Kudlick, M.D., 1966. On transient motions in a contained, rotating fluid, *PhD thesis*, Massachusetts Institute of Technology.
Landau, L.D. & Lifshitz, E.M., 1977. *Quantum Mechanics*, 3rd edn, Pergamon Press, Oxford.
Lecolazet, R. & Steinmetz, L., 1974. Sur les ondes diurnes de la marée gravimétrique observée à Strasbourg, *C.R. Acad. Sc. Paris,* **278,** 295–297.
Lecolazet, R. & Melchior, P., 1977. Experimental determination of the dynamical effects of the liquid core of the Earth, *Ann. Geophys.,* **33,** 11–22.
Longuet-Higgins, M.S., 1964. Planetary waves on a rotating plane, *Proc. Roy. Soc. A,* **279,** 446–473.
Lumb, L.I. & Aldridge, K.D., 1991. On viscosity estimates for the Earth's fluid outer core and core-mantle coupling, *J. Geomag. Geoelectr.,* **43,** 93–110.
MacKay, R.S. & Saffman, P.G., 1986. Stability of water waves, *Proc. R. Soc. Lond.*, **A 406,** 115–125.
Masters, G., 1979. Observational constraints on the chemical and thermal structure of the Earth's deep interior, *Geophys. J. R. astr. Soc.,* **57,** 507–534.
Mathews, P.M., Buffett, B.A., Herring, T.A. & Shapiro, I.I., 1991. Forced nutations of the Earth: influence of inner core dynamics, 1. Theory, *J. geophys. Res.,* **96,** 8219–8242.
Mathews, P.M., Herring, T.A. & Buffett, B.A., 2002. Modeling of nutation and precession: new nutation series for nonrigid Earth and insights into the Earth's interior, *J. geophys. Res.,* **107**(B4), 2068, doi:10.1029/2001JB000390.
Molodensky, M.S., 1961. The theory of nutation and diurnal Earth tides, *Comm. Obs. R. Belgique,* **58,** 25–56.
Pan, C., 2007. The observed multiple frequencies of the Chandler wobble, *J. Geodyn.,* **44,** 47–65.
Poincaré, H., 1910. Sur la précession des corps déformables, *Bull. Astron.,* **27,** 321–356.
Ralston, J.V., 1973. On stationary modes in inviscid rotating fluids, *J. Math. Anal. Appl.,* **44,** 366–383.
Rieutord, M., 1991. Linear theory of rotating fluids using spherical harmonics – Part II: Time-periodic flows, *Geophys. Astrophys. Fluid Dynamics,* **59,** 185–208.
Rieutord, M. & Valdaretto, L., 1997. Inertial waves in a rotating spherical shell, *J. Fluid Mech.,* **341,** 77–99.
Rieutord, M., Georgeot, B. & Valdettaro, L., 2001. Inertial waves in a rotating spherical shell: attractors and asymptotic spectrum, *J. Fluid Mech.,* **435,** 103–144.
Rochester, M.G., Jensen, O.G. & Smylie, D.E., 1974. A search for the Earth's 'Nearly Diurnal Free Wobble', *Geophys. J. R. astr. Soc.,* **38,** 349–363.
Rogister, Y., 2001. On the diurnal and nearly diurnal free modes of the Earth, *Geophys. J. Int.,* **144,** 459–470.
Rogister, Y., 2003. Splitting of seismic free oscillations and of the Slichter triplet using the normal mode theory of a rotating, ellipsoidal Earth, *Phys. Earth planet. Inter.,* **140,** 169–182.
Rogister, Y. & Rochester, M.G., 2004. Normal-mode theory of a rotating Earth model using a Lagrangian perturbation of a spherical model of reference, *Geophys. J. Int.,* **159,** 874–908.
Rogister, Y. & Valette, B., 2005. Influence of outer core dynamics on Chandler wobble, in *Forcing of Polar Motion in the Chandler Frequency Band: A Contribution to Understanding Interannual Climate Variations*,Vol. 24, pp. 61–68, eds Plag, H.-P., Chao, B., Gross, R. & Van Dam, T., Cahiers du Centre Européen de Géodynamique et de Séismologie.
Rotter, I., 2001. Dynamics of quantum systems, Phys. Rev. E, **64,** 1–12.
Sasao, T., Okubo, S. & Saito, M., 1980. A simple theory on the dynamical effects of a stratified fluid core upon nutational motion of the Earth, in *Nutation and the Earth's Rotation*, pp. 165–183, eds Fedorov, E.P., Smith, M.L. & Bender, P.L., Dordrecht, Netherlands: Reidel.
Schastok, J., 1997. A new nutation series for a more realistic model Earth, *Geophys. J. Int.,* **130,** 137–150.

Schwarzschild, K., 1906. Über das Gleichgewicht der Sonneatmosphäre [On the equilibrium of the Sun's atmosphere], *Göttingen Nachr.,* **1,** 41.

Smith, M.L., 1974. The scalar equations of infinitesimal elastic-gravitational motion for a rotating, slightly elliptical Earth, *Geophys. J. R. astr. Soc.,* **37,** 491–526.

Smith, M.L., 1977. Wobble and nutation of the Earth, *Geophys. J. R. astr. Soc.,* **50,** 103–140.

Smith, M.L. & Dahlen, F.A., 1981. The period and Q of the Chandler wobble, *Geophys. J. R. astr. Soc.,* **64,** 223–281.

Stefani, F., Gerbeth, G., Günther, U. & Xu, M., 2006. Why dynamos are prone to reversals, *Earth planet. Sci. Lett.,* **243,** 828–840.

Toomre, A., 1974. On the 'Nearly Diurnal Wobble' of the Earth, *Geophys. J. R. astr. Soc.,* **38,** 335–348.

Valette, B., 1986. About the influence of pre-stress upon adiabatic perturbations of the Earth, *Geophys. J. R. astr. Soc.,* **85,** 179–208.

Valette, B., 1989a. Spectre des vibrations propres d'un corps élastique, autogravitant, en rotation uniforme et contenant une partie fluide, *C. R. Acad. Sci. Paris,* **309,** Sér. I, 419–422.

Valette, B., 1989b. Etude d'une classe de problèmes spectraux, *C. R. Acad. Sci. Paris,* **309,** Sér. I, 785–788.

Wu, W.J. & Rochester, M.G., 1993. Computing core oscillation eigenperiods for the rotating Earth: a test of the subseismic approximation, *Phys. Earth planet. Int.,* **78,** 33–50.

Wu, X. & Wahr, J.M., 1997. Effects of non-hydrostatic core–mantle boundary topography and core dynamics on Earth rotation, *Geophys. J. Int.,* **128,** 18–42.